

Fixed time event-triggered control for high-order nonlinear uncertain systems with time-varying state constraints

Panpan Yang¹, Xuyang Wang¹, Xingwen Chen², and dusen du¹

¹Chang'an University

²Harbin Institute of Technology

December 28, 2022

Abstract

The fixed time event-triggered control for high-order nonlinear uncertain systems with time-varying state constraints is investigated in this paper. First, the event-triggered control (ETC) mechanism is introduced to reduce data transmission in the communication channel. In consideration of the physical constraints and engineering requirements, time-varying barrier Lyapunov function (BLF) is deployed to make the system states confined in the given time-varying constraints. Then, the radial basis function neural networks (RBF NNs) is used to approximate the unknown nonlinear terms. Further, the fixed time stability strategy is deployed to make the system achieve semiglobal practical fixed time stability (SPFTS) and the convergence time is independent of the initial conditions. Finally, the proposed control scheme is verified by two simulation examples.

ARTICLE TYPE

Fixed time event-triggered control for high-order nonlinear uncertain systems with time-varying state constraints

Panpan Yang¹ | Xuyang Wang¹ | Xingwen Chen² | Sen Du¹

¹School of Electronics and Control Engineering, Chang'an University, Xi'an, China

²Research Institute of Intelligent Control and Systems, Harbin Institute of Technology, Harbin, China.

Correspondence

Panpan Yang, School of Electronics and Control Engineering, Chang'an University, Xi'an, China

Email: panpanyang@chd.edu.cn

Present Address

This work was supported by the Key Research and Development Plan of China (No. 2021YFA1000303), the National Natural Science Foundation of China (No. 61803040), the Key Research and Development Plan of Shaanxi Province (No. 2022GY-255), and the Fundamental Research Funds for the Central University of China (No. 300102320203).

Summary

The fixed time event-triggered control for high-order nonlinear uncertain systems with time-varying state constraints is investigated in this paper. First, the event-triggered control (ETC) mechanism is introduced to reduce data transmission in the communication channel. In consideration of the physical constraints and engineering requirements, time-varying barrier Lyapunov function (BLF) is deployed to make the system states confined in the given time-varying constraints. Then, the radial basis function neural networks (RBF NNs) is used to approximate the unknown nonlinear terms. Further, the fixed time stability strategy is deployed to make the system achieve semiglobal practical fixed time stability (SPFTS) and the convergence time is independent of the initial conditions. Finally, the proposed control scheme is verified by two simulation examples.

KEYWORDS:

high-order nonlinear systems, event-triggered control, fixed-time stability, time-varying state constraints

1 | INTRODUCTION

In the last few decades, the control of high-order nonlinear systems has attracted considerable attention for its ever increasing applications in practical engineering, such as sliding mode control for aerial devices, robust following control for autonomous underwater vehicles, structured robust synthesis control for flexible aircraft flutter suppression, and etc. [1-3] Generally, high-order nonlinear systems are composed of multiple subsystems with complex cross-couplings, [4] and they are also suffering from nonlinear characteristics, uncertainties and external disturbances, [5] which enhances the difficulty in the control of high-order nonlinear systems.

For high-order nonlinear systems, the output feedback control was presented based on various Lyapunov equations in [6]. In [7], Nikiforov *et al.* proposed a modular backstepping design for new high-order tuner to improve the transient performance. In [8], Zhang *et al.* considered the cooperative tracking control problem of networked higher-order nonlinear systems with distinct unknown dynamics and bounded external disturbances. In addition, for the nonlinear and uncertain terms in high-order nonlinear system, Yang *et al.* utilized the radial basis function neural networks (RBF NNs) to design the state observer and approximate the unknown nonlinear function in [9]. In [10], the neural networks were employed to approximate unknown interconnected terms and nonlinear functions. In [11], Yang *et al.* proposed a pinning adaptive coupling method to ensure global synchronization without knowing the bound of parameter uncertainties.

⁰**Abbreviations:** ANA, anti-nuclear antibodies; APC, antigen-presenting cells; IRF, interferon regulatory factor

Convergence time is an important concern in some practical control systems, [12] finite-time control is usually utilised for faster convergence rate and better transient performance. [13-15] However, the convergence time of finite-time control depends on the system initial conditions, which may not meet some critical requirements. [16] Fixed time control, whose convergence time is a predetermined value, has been regarded as a promising alternative for critical transient requirements. In the work of [17], fixed time stability of the positive nonlinear systems was guaranteed by a Lyapunov function based criterion. In [18], Du *et al.* designed distributed fixed time observers and fixed time tracking controllers to make the heterogeneous nonlinear multi-agent systems achieve distributed consensus in a fixed time. In [19], dynamic gain control approach and fixed time distributed observer was used to design a new dynamic controller with two online tuned gains. A new fixed time stable criterion is established in [20], which provides an efficient tool for the fixed time control in the fuzzy control framework. In [21], Wang *et al.* investigated the fixed time containment control of second-order nonlinear multi-agent systems.

Time-triggered control is frequently used in the control system design for satisfactory control performance. [15] However, such periodic sampling will inevitably cause network redundancy and computing resources waste due to the limited bandwidth and the restriction of onboard energy. The event-triggered control(ETC), where the control task is executed only when the triggering condition is violated,[22] has received considerable attention for communication resources saving. [23-26] Qin *et al.* [23] proposed an observer-based event-triggered fuzzy control strategy, which can ensure the stability of the closed-loop system and make the tracking error converge to arbitrary small value. In [24], Sun *et al.* proposed an adaptive fuzzy event-triggered tracking control approach, which not only ensures that the tracking error is always within a predefined region but also reduces the communication burden from the controller to the actuator. In [25], a novel event-triggered mechanism is proposed to determine when data needs to be transferred. Yang *et al.* investigated a tracking error-based event-triggered strategy to reduce the data transmission in [26].

It is well known that there are many constraints in practical control systems due to the performance requirement or the physical characteristics. [27] The violation of constraints may lead to the system instability or even damage the system. To this end, the constrained state estimator was derived based on the projection method and the unconstrained linear minimum mean square error estimator in [28]. In [29], a simple derivation based on stochastic arguments of the covariance of the constrained Kalman filter for time-variant systems was presented. In [30], Keng *et al.* presented the control design based on the barrier Lyapunov function(BLF) for strict feedback systems with an output constraint. In [31], an adaptive output feedback control via command filtered backstepping was proposed for a class of uncertain nonlinear systems with full-state constraints. For the time-varying state constraints, an adaptive neural network controller is constructed by introducing the asymmetric time-varying BLF, which ensures that the states do not violate the asymmetric time-varying constraint regions. [32] In [33], time-varying BLF was used to ensure that the constrained subsystems will not violate the time-varying constraint. In [34], a novel time-varying BLF-based adaptive fuzzy backstepping control scheme is designed for the uncertain nonstrict-feedback nonlinear systems to realize superior tracking performances and keep the states staying in predefined time-varying compact regions.

Motivated by the above descriptions, the fixed time event-triggered control for high-order nonlinear uncertain systems with time-varying state constraints is investigated in this paper. The main contributions of this paper are summarized as follows.

- 1) Compared with the finite time stability, the fixed time stability theory introduced in this paper can make the system have faster convergence rate and the convergence time is not affected by the initial conditions.
- 2) Different from the time-triggered method of periodic sampling, the event-triggered control proposed in this paper can reduce unnecessary information transmission and save network resources greatly.
- 3) Compared with literature [27, 30-31], time-varying BLF adopted in this paper solves the problem of time-varying constraints for high-order nonlinear uncertain systems, which is more universal and practical.

The remainder of this paper is as follows. Section II gives preliminary knowledge and problem formulation. Then, the design of the control scheme and fixed time stability analysis are shown in Section III. Section IV presents two representative simulation examples. Finally, Section V concludes this paper.

2 | PRELIMINARY AND PROBLEM FORMULATION

2.1 | Definition and lemmas

Consider the following system

$$\dot{x} = f(x), x(0) = x_0, \quad (1)$$

where $x \in \mathbb{R}^n$ is the system state, $f : \mathbb{R}_+ \times \mathbb{R}^n \rightarrow \mathbb{R}^n$ is a nonlinear function.

Definition 1. [9] System (1) is called semiglobal practical fixed time stable (SPFSTS) if it is globally asymptotically stable and any solutions of (1) converge to the origin within the time T_f bounded by T_{\max} , i.e. $\exists T_{\max}, T_f(x_0) < T_{\max}$.

Lemma 1. [9] If there exists some positive constants $P > 0, Q > 0, 0 < \alpha_1 < 1, \alpha_2 > 1$ and $0 < \beta < \infty$ and a selected Lyapunov function $V(x)$ such that

$$\dot{V}(x) \leq -PV^{\alpha_1}(x) - QV^{\alpha_2}(x) + \beta \quad (2)$$

then the trajectory of system (1) is semiglobal practical fixed time stable and the states of system (1) can reach the following set within the interval $[0, T_f]$

$$\Omega = \left\{ x \mid V(x) \leq \min \left\{ \left(\frac{\beta}{P(1-\iota)} \right)^{\frac{1}{\alpha_1}}, \left(\frac{\beta}{Q(1-\iota)} \right)^{\frac{1}{\alpha_2}} \right\} \right\}$$

where the scalar ι satisfies $0 < \iota < 1$, and the time T_f is bounded by the fixed-time T_{\max}

$$T_f \leq T_{\max} = \frac{1}{P\iota(1-\alpha_1)} + \frac{1}{Q\iota(\alpha_2-1)} \quad (3)$$

Lemma 2. [22] For any real variables κ and χ , any positive constants a, b and s , one has

$$|\kappa|^a |\chi|^b \leq \frac{a}{a+b} s |\kappa|^{a+b} + \frac{b}{a+b} s^{-\frac{a}{b}} |\chi|^{a+b} \quad (4)$$

Lemma 3. [22] For $\forall(\kappa, \chi) \in \mathbb{R}^2$, the following inequality holds

$$\kappa \chi \leq \frac{\tau^p}{p} |\kappa|^p + \frac{1}{q\tau^q} |\chi|^q \quad (5)$$

with $\tau > 0, p > 1, q > 1$ and $(p-1)(q-1) = 1$.

Lemma 4. [22] For $\zeta_1, \zeta_2, \dots, \zeta_n \geq 0$ and $d > 0$, if $0 < d < 1$, one has

$$\sum_{i=1}^n \zeta_i^d \geq \left(\sum_{i=1}^n \zeta_i \right)^d$$

else

$$\sum_{i=1}^n \zeta_i^d \geq n^{1-d} \left(\sum_{i=1}^n \zeta_i \right)^d \quad (6)$$

Lemma 5. [22] For any $\varpi \in \mathbb{R}$ and $\mu > 0$, the following inequation holds

$$0 \leq |\varpi| - \varpi \tanh \left(\frac{\varpi}{\mu} \right) \leq 0.2785\mu \quad (7)$$

In this paper, the radial basis function neural networks (RBF NNs) will be utilised to approximate some unknown continuous nonlinear functions. Therefore, some preliminaries on RBF NNs are given.

Lemma 6. [9] The RBF NNs can be expressed by

$$\varphi(Z) = W^T S(Z) = \sum_{i=1}^m w_i s_i(Z) \quad (8)$$

$$s_i(Z) = \exp\left(-\frac{\|Z - c_i\|^2}{b_i^2}\right) \quad (9)$$

where $\varphi(Z)$ is the output of the RBF NNs, $Z = [z_1, \dots, z_n]^T$ is the input vector, $m > 0$ is the number of RBF NNs nodes, $W = [w_1, \dots, w_m]^T$ is the weight vector. $s_i(Z)$ is the Gaussian function, b_i is the width of the Gaussian function, $c_i = [c_{i1}, \dots, c_{in}]^T$ is central point vector value of the i -th cryptic neuron.

Then, the unknown nonlinear function $f(Z)$ can be approximated by the RBF NNs as

$$f(Z) = W^* S(Z) + \Delta(Z) \quad (10)$$

where $\Delta(Z)$ is approximation error satisfying $|\Delta(Z)| \leq \varepsilon$.

2.2 | Problem description

Consider the high-order nonlinear uncertain system composed of N subsystems with n_i th-order nonlinear dynamics. The dynamics of i th subsystem can be described as

$$\begin{cases} \dot{x}_{i,j}(t) = x_{i,j+1}(t) + f_{i,j} + \omega_{i,j}, j = 1, \dots, n_i - 1 \\ \dot{x}_{i,n_i}(t) = u_i(t) + f_{i,n_i} + \omega_{i,n_i}, \\ y_i(t) = x_{i,1}(t), i = 1, 2, \dots, N. \end{cases} \quad (11)$$

where $x_i = [x_{i,1}, x_{i,2}, \dots, x_{i,n_i}] \in \mathbb{R}^{n_i}$, $u_i \in \mathbb{R}$, $y_i \in \mathbb{R}$ are system states, control input, and system output, respectively. $f_{i,j}$ ($j = 1, 2, \dots, n_i$) is the unknown smooth nonlinear function. $\omega_{i,j}$ ($j = 1, \dots, n_i$) denotes the unknown time-varying external disturbances.

The purpose of this paper is to design the control input u_i for the i th high-order nonlinear subsystem (11), such that

- 1) The output $y_i(t)$ can track the reference signal $y_{i,d}$ within the fixed time and all the closed-loop signals are SPFTS.
- 2) The communication resources are significantly reduced with the introduction of the event-triggered mechanism.
- 3) All states of the system are constrained in a time-varying function, which is more practical in applications.

Before the controller design, some useful assumptions are presented.

Assumption 1. The desired reference signal $y_{i,d}(t)$ and its time derivatives up to the n_i th order are continuous and bounded.

Assumption 2. The external disturbances $\omega_{i,j}(t)$ ($j = 1, 2, \dots, n_i$) are bounded with unknown positive upper bounds $\bar{\omega}_{i,j}$, i.e., $|\omega_{i,j}(t)| \leq \bar{\omega}_{i,j}$.

3 | MAIN RESULTS

In this section, a fixed time event-triggered controller with state constraints is designed via the backstepping technique. The architecture of the control scheme is shown in Fig. 1. Firstly, RBF NNs is adopted to approximate the nonlinear and uncertain terms in the system. Meanwhile, fixed time stability is adopted to make convergence time independent of initial value, and time-varying BLF is adopted to handle time-varying state constraints. Then, ETC is used in controller design to reduce unnecessary information transmission. Finally, the control signal is transmitted to the subsystem through the network to fulfill the control task.

3.1 | Event-triggered mechanism

In this paper, the event-triggered mechanism (ETM) is introduced to save communication resources. The control input $u_i(t)$ of system (11) will update when the preset condition is violated. Hence, the event-triggered condition is determined by

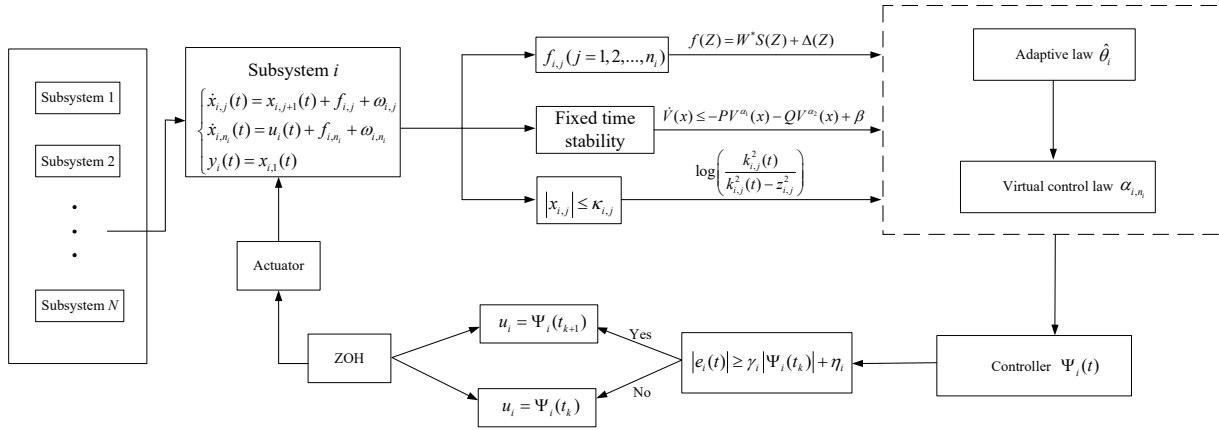


FIGURE 1 Architecture of the fixed time event-triggered control scheme with state constraints

$$|e_i(t)| \geq \gamma_i |\Psi_i(t_k)| + \eta_i \quad (12)$$

where $e_i(t) = \Psi_i(t) - \Psi_i(t_k)$ and $\Psi_i(t)$, $\Psi_i(t_k)$ are control signals at the current time and the previous triggering instant, respectively. $\gamma_i \in (0, 1)$ and $\eta_i > 0$ are two positive parameters to be designed. And the triggering instant can be represented by

$$t_{k+1} = \inf \left\{ t > t_k \mid |e_i(t)| \geq \gamma_i |\Psi_i(t_k)| + \eta_i \right\} \quad (13)$$

According to the ETM, the control signal $\Psi_i(t)$ can be written as

$$\Psi_i(t) = (1 + \varsigma_1(t)\gamma_i) u_i(t) + \varsigma_2(t)\eta_i, \quad t \in [t_k, t_{k+1}) \quad (14)$$

where $\varsigma_1(t)$ and $\varsigma_2(t)$ are time-varying parameters with $|\varsigma_1(t)| \leq 1$ and $|\varsigma_2(t)| \leq 1$.

Then, $u_i(t)$ can be rewritten as

$$u_i(t) = \frac{\Psi_i(t)}{1 + \varsigma_1(t)\gamma_i} - \frac{\varsigma_2(t)\eta_i}{1 + \varsigma_1(t)\gamma_i} \quad (15)$$

Remark 1. Different from the fixed triggering threshold in [23], the proposed event-triggered strategy in (13) is based on the relative threshold, by which the system can automatically adjust the triggering threshold for better control performance.

Remark 2. The event-triggered controller based on the relative threshold strategy is to design a time-varying threshold associated with the control signal $\psi_i(t_k)$ of the previous triggering instant. When $\psi_i(t_k)$ is large, the control tasks are executed under a big threshold to avoid frequent triggering. When $\psi_i(t_k)$ is small, a small threshold will be produced to acquire more precise control and get better control performance.

3.2 | Fixed time event-triggered controller design

In order to design the fixed time controller, the coordinate transformation based on backstepping technique is given as

$$\begin{cases} z_{i,1} = x_{i,1} - y_{i,d}, \\ z_{i,m} = x_{i,m} - \alpha_{i,m-1}, m = 2, \dots, n_i. \end{cases} \quad (16)$$

where $z_{i,m}$ ($m = 1, 2, \dots, n_i$) are tracking errors, $y_{i,d}$ is the desired reference signal and $\alpha_{i,m}$ ($m = 1, 2, \dots, n_i$) are virtual control laws.

Step i , 1: Consider the tracking error $z_{i,1} = x_{i,1} - y_{i,d}$, its time derivative is

$$\dot{z}_{i,1} = \dot{x}_{i,1} - \dot{y}_{i,d} = x_{i,2} + f_{i,1} + \omega_{i,1} - \dot{y}_{i,d} \quad (17)$$

For the time-varying state constraints, the time-varying function $k_{i,1}(t)$ is defined as

$$k_{i,1}(t) = (k_{1a} - k_{1b})e^{-l_1 t} + k_{1b} \quad (18)$$

where k_{1a} , k_{1b} and l_1 are constants satisfying $k_{1a} > k_{1b} > 0$ and $l_1 > 0$. Obviously, the time-varying function $k_{i,1}(t)$ is positive bounded and differentiable and $k_{1b} < k_{i,1}(t) < k_{1a}$ holds.

Choose the following Barrier Lyapunov function as

$$V_{i,1} = \frac{1}{2} \log \frac{k_{i,1}^2(t)}{k_{i,1}^2(t) - z_{i,1}^2} \quad (19)$$

Taking the time derivative of $V_{i,1}$ yields

$$\dot{V}_{i,1} = \frac{z_{i,1}}{h_{i,1}} \dot{z}_{i,1} + \frac{\dot{k}_{i,1}}{k_{i,1}} - \frac{k_{i,1} \dot{k}_{i,1}}{h_{i,1}} = \frac{z_{i,1}}{h_{i,1}} (x_{i,2} + f_{i,1} + \omega_{i,1} - \dot{y}_{i,d}) + \frac{\dot{k}_{i,1}}{k_{i,1}} - \frac{k_{i,1} \dot{k}_{i,1}}{h_{i,1}} \quad (20)$$

where $h_{i,1} = k_{i,1}^2(t) - z_{i,1}^2$

According to Lemma 3, one has

$$\frac{z_{i,1}}{h_{i,1}} \omega_{i,1} \leq \frac{z_{i,1}^2}{2h_{i,1}^2} + \frac{1}{2} \bar{\omega}_{i,1}^2 \quad (21)$$

Substituting (21) into (20) yields

$$\begin{aligned} \dot{V}_{i,1} &\leq \frac{z_{i,1}}{h_{i,1}} (x_{i,2} + f_{i,1} - \dot{y}_{i,d}) + \frac{z_{i,1}^2}{2h_{i,1}^2} + \frac{1}{2} \bar{\omega}_{i,1}^2 + \frac{\dot{k}_{i,1}}{k_{i,1}} - \frac{k_{i,1} \dot{k}_{i,1}}{h_{i,1}} \\ &= \frac{z_{i,1}}{h_{i,1}} (x_{i,2} + \varphi_{i,1} - \dot{y}_{i,d}) + \frac{z_{i,1}^2}{2h_{i,1}^2} + \frac{1}{2} \bar{\omega}_{i,1}^2 + \frac{\dot{k}_{i,1}}{k_{i,1}} - \frac{k_{i,1} \dot{k}_{i,1}}{h_{i,1}} \end{aligned} \quad (22)$$

where $\varphi_{i,1} \triangleq f_{i,1}$.

According to Lemma 7, the RBF NNs can approximate $\varphi_{i,1}$ as

$$\varphi_{i,1} = W_{i,1}^T S_{i,1} + \Delta_{i,1} \quad (23)$$

where $\Delta_{i,1}$ is the approximation error satisfying $|\Delta_{i,1}| \leq \varepsilon_{i,1}$ with $\varepsilon_{i,1} > 0$.

According to Lemma 3, one has

$$\frac{z_{i,1}}{h_{i,1}} \varphi_{i,1} \leq \frac{|z_{i,1}|}{h_{i,1}} (\|W_{i,1}\| \|S_{i,1}\| + \varepsilon_{i,1}) \leq \frac{z_{i,1}^2}{2c_{i,1}^2 h_{i,1}^2} \|W_{i,1}\|^2 S_{i,1}^T S_{i,1} + \frac{1}{2} c_{i,1}^2 + \frac{z_{i,1}^2}{2h_{i,1}^2} + \frac{1}{2} \varepsilon_{i,1}^2 \quad (24)$$

where $c_{i,1}$ is a positive parameter to be designed.

Substituting (24) into (22), the following inequality can be obtained

$$\dot{V}_{i,1} \leq \frac{z_{i,1}}{h_{i,1}} (x_{i,2} - \dot{y}_{i,d}) + \frac{z_{i,1}^2}{h_{i,1}^2} + \frac{\dot{k}_{i,1}}{k_{i,1}} - \frac{k_{i,1} \dot{k}_{i,1}}{h_{i,1}} + \frac{z_{i,1}^2}{2c_{i,1}^2 h_{i,1}^2} \|W_{i,1}\|^2 S_{i,1}^T S_{i,1} + \frac{1}{2} \bar{\omega}_{i,1}^2 + \frac{1}{2} c_{i,1}^2 + \frac{1}{2} \varepsilon_{i,1}^2 \quad (25)$$

For the convenience of calculation, define the estimation error $\tilde{\theta}_i$ as

$$\tilde{\theta}_i = \theta_i - \hat{\theta}_i \quad (26)$$

where $\theta_i = \max \{\|W_{i,j}\|^2, j = 1, 2, \dots, n_i\}$, and $\hat{\theta}_i$ is the estimation of θ_i .

Construct the virtual control law $\alpha_{i,1}$ as

$$\alpha_{i,1} = -g_{i11} \frac{z_{i,1}^{\rho_1}}{h_{i,1}^{\frac{\rho_1-1}{2}}} - g_{i12} \frac{z_{i,1}^{\rho_2}}{h_{i,1}^{\frac{\rho_2-1}{2}}} - \frac{2z_{i,1}}{h_{i,1}} - \dot{k}_{i,1} - \frac{z_{i,1}}{2c_{i,1}^2 h_{i,1}} \hat{\theta}_i S_{i,1}^T S_{i,1} + \dot{y}_{i,d} \quad (27)$$

where $g_{i11} > 0$, $g_{i12} > 0$, $0 < \rho_1 < 1$, $\rho_2 > 1$ are parameters to be designed.

Substituting the virtual control law $\alpha_{i,1}$ into (25) yields

$$\begin{aligned}
\dot{V}_{i,1} &\leq -g_{i11} \frac{z_{i,1}^{\rho_1+1}}{h_{i,1}^{\frac{\rho_1+1}{2}}} - g_{i12} \frac{z_{i,1}^{\rho_2+1}}{h_{i,1}^{\frac{\rho_2+1}{2}}} - \frac{2z_{i,1}^2}{h_{i,1}^2} - \frac{z_{i,1}}{h_{i,1}} \dot{k}_{i,1} - \frac{z_{i,1}^2}{2c_{i,1}^2 h_{i,1}^2} \hat{\theta}_i S_{i,1}^T S_{i,1} + \frac{z_{i,1}}{h_{i,1}} (x_{i,2} - \alpha_{i,1}) + \frac{z_{i,1}^2}{h_{i,1}^2} + \frac{\dot{k}_{i,1}}{k_{i,1}} - \frac{k_{i,1} \dot{k}_{i,1}}{h_{i,1}} \\
&\quad + \frac{z_{i,1}^2}{2c_{i,1}^2 h_{i,1}^2} \|W_{i,1}\|^2 S_{i,1}^T S_{i,1} + \frac{1}{2} \bar{\omega}_{i,1}^2 + \frac{1}{2} c_{i,1}^2 + \frac{1}{2} \epsilon_{i,1}^2 \\
&= -g_{i11} \frac{z_{i,1}^{\rho_1+1}}{h_{i,1}^{\frac{\rho_1+1}{2}}} - g_{i12} \frac{z_{i,1}^{\rho_2+1}}{h_{i,1}^{\frac{\rho_2+1}{2}}} - \frac{z_{i,1}^2}{h_{i,1}^2} + \frac{z_{i,1}}{h_{i,1}} \left(-\dot{k}_{i,1} - \frac{k_{i,1} \dot{k}_{i,1}}{z_{i,1}} \right) + \frac{\dot{k}_{i,1}}{k_{i,1}} + \frac{z_{i,1}}{h_{i,1}} (x_{i,2} - \alpha_{i,1}) \\
&\quad + \frac{z_{i,1}^2}{2c_{i,1}^2 h_{i,1}^2} (\|W_{i,1}\|^2 - \hat{\theta}_i) S_{i,1}^T S_{i,1} + \frac{1}{2} \bar{\omega}_{i,1}^2 + \frac{1}{2} c_{i,1}^2 + \frac{1}{2} \epsilon_{i,1}^2
\end{aligned} \tag{28}$$

Utilizing Lemma 3, one can get

$$\frac{z_{i,1}}{h_{i,1}} \left(-\dot{k}_{i,1} - \frac{k_{i,1} \dot{k}_{i,1}}{z_{i,1}} \right) = -\dot{k}_{i,1} \frac{z_{i,1}}{h_{i,1}} \left(1 + \frac{k_{i,1}}{z_{i,1}} \right) \leq -2\dot{k}_{i,1} \frac{|z_{i,1}|}{h_{i,1}} \leq \frac{z_{i,1}^2}{h_{i,1}^2} + (\dot{k}_{i,1})^2 \tag{29}$$

From the definition of $k_{i,1}$ in (18), we know that $k_{i,1}$ and $\dot{k}_{i,1}$ are bounded. Furthermore, it follows that

$$\frac{\dot{k}_{i,1}}{k_{i,1}} + (\dot{k}_{i,1})^2 \leq K_{i,1} \tag{30}$$

where $K_{i,1}$ is a positive constant.

Substituting (29)-(30) into (28), one has

$$\dot{V}_{i,1} \leq -g_{i11} \frac{z_{i,1}^{\rho_1+1}}{h_{i,1}^{\frac{\rho_1+1}{2}}} - g_{i12} \frac{z_{i,1}^{\rho_2+1}}{h_{i,1}^{\frac{\rho_2+1}{2}}} + \frac{z_{i,1}}{h_{i,1}} (x_{i,2} - \alpha_{i,1}) + \frac{z_{i,1}^2}{2c_{i,1}^2 h_{i,1}^2} (\|W_{i,1}\|^2 - \hat{\theta}_i) S_{i,1}^T S_{i,1} + K_{i,1} + \frac{1}{2} \bar{\omega}_{i,1}^2 + \frac{1}{2} c_{i,1}^2 + \frac{1}{2} \epsilon_{i,1}^2 \tag{31}$$

Step i, m ($m = 2, \dots, n_i - 1$): Consider the tracking error $z_{i,m} = x_{i,m} - \alpha_{i,m-1}$, its time derivative is

$$\dot{z}_{i,m} = \dot{x}_{i,m} - \dot{\alpha}_{i,m-1} = x_{i,m+1} + f_{i,m} + \omega_{i,m} - \dot{\alpha}_{i,m-1} \tag{32}$$

Define the time-varying function $k_{i,m}(t)$ as

$$k_{i,m}(t) = (k_{ma} - k_{mb})e^{-l_m t} + k_{mb} \tag{33}$$

where constants $k_{ma} > k_{mb} > 0$ and $l_m > 0$. Obviously, the time-varying function $k_{i,m}(t)$ is positive bounded and differentiable and $k_{mb} < k_{i,m}(t) < k_{ma}$ holds.

Choose the following Barrier Lyapunov function as

$$V_{i,m} = V_{i,m-1} + \frac{1}{2} \log \frac{k_{i,m}^2(t)}{k_{i,m}^2(t) - z_{i,m}^2} \tag{34}$$

The time derivative of $V_{i,m}$ is obtained as

$$\dot{V}_{i,m} = \dot{V}_{i,m-1} + \frac{z_{i,m}}{h_{i,m}} (x_{i,m+1} + f_{i,m} + \omega_{i,m} - \dot{\alpha}_{i,m-1}) + \frac{\dot{k}_{i,m}}{k_{i,m}} - \frac{k_{i,m} \dot{k}_{i,m}}{h_{i,m}} \tag{35}$$

where $h_{i,m} = k_{i,m}^2(t) - z_{i,m}^2$.

According to Lemma 3, one has

$$\frac{z_{i,m}}{h_{i,m}} \omega_{i,m} \leq \frac{z_{i,m}^2}{2h_{i,m}^2} + \frac{1}{2} \bar{\omega}_{i,m}^2 \tag{36}$$

Substituting (36) into (35), one has

$$\begin{aligned}
\dot{V}_{i,m} &\leq \dot{V}_{i,m-1} + \frac{z_{i,m}}{h_{i,m}} (x_{i,m+1} + f_{i,m} - \dot{\alpha}_{i,m-1}) + \frac{z_{i,m}^2}{2h_{i,m}^2} + \frac{1}{2}\bar{\omega}_{i,m}^2 + \frac{\dot{k}_{i,m}}{k_{i,m}} - \frac{k_{i,m}\dot{k}_{i,m}}{h_{i,m}} \\
&= -\sum_{j=1}^{m-1} g_{ij1} \frac{z_{i,j}^{\rho_1+1}}{h_{i,j}^{\frac{\rho_1+1}{2}}} - \sum_{j=1}^{m-1} g_{ij2} \frac{z_{i,j}^{\rho_2+1}}{h_{i,j}^{\frac{\rho_2+1}{2}}} + \sum_{j=1}^{m-1} \frac{z_{i,j}^2}{2c_{i,j}^2 h_{i,j}^2} (\|W_{i,j}\|^2 - \hat{\theta}_i) S_{i,j}^T S_{i,j} + \sum_{j=1}^{m-1} K_{i,j} + \frac{1}{2} \sum_{j=1}^{m-1} (c_{i,j}^2 + \varepsilon_{i,j}^2 + \bar{\omega}_{i,j}^2) \\
&\quad + \frac{z_{i,m}^2}{2h_{i,m}^2} + \frac{z_{i,m}}{h_{i,m}} \left(x_{i,m+1} + \frac{z_{i,m-1} h_{i,m}}{h_{i,m-1}} + f_{i,m} - \dot{\alpha}_{i,m-1} \right) + \frac{\dot{k}_{i,m}}{k_{i,m}} - \frac{k_{i,m}\dot{k}_{i,m}}{h_{i,m}} + \frac{1}{2}\bar{\omega}_{i,m}^2 \\
&= -\sum_{j=1}^{m-1} g_{ij1} \frac{z_{i,j}^{\rho_1+1}}{h_{i,j}^{\frac{\rho_1+1}{2}}} - \sum_{j=1}^{m-1} g_{ij2} \frac{z_{i,j}^{\rho_2+1}}{h_{i,j}^{\frac{\rho_2+1}{2}}} + \sum_{j=1}^{m-1} \frac{z_{i,j}^2}{2c_{i,j}^2 h_{i,j}^2} (\|W_{i,j}\|^2 - \hat{\theta}_i) S_{i,j}^T S_{i,j} + \sum_{j=1}^{m-1} K_{i,j} + \frac{1}{2} \sum_{j=1}^{m-1} (c_{i,j}^2 + \varepsilon_{i,j}^2 + \bar{\omega}_{i,j}^2) \\
&\quad + \frac{z_{i,m}^2}{2h_{i,m}^2} + \frac{z_{i,m}}{h_{i,m}} (x_{i,m+1} + \varphi_{i,m}) + \frac{\dot{k}_{i,m}}{k_{i,m}} - \frac{k_{i,m}\dot{k}_{i,m}}{h_{i,m}} + \frac{1}{2}\bar{\omega}_{i,m}^2
\end{aligned} \tag{37}$$

where $\varphi_{i,m} \triangleq \frac{z_{i,m-1} h_{i,m}}{h_{i,m-1}} + f_{i,m} - \dot{\alpha}_{i,m-1}$.

According to Lemma 7, $\varphi_{i,m}$ can be approximated by RBF NNs as

$$\varphi_{i,m} = W_{i,m}^T S_{i,m} + \Delta_{i,m} \tag{38}$$

where $\Delta_{i,m}$ is the approximation error satisfying $|\Delta_{i,m}| \leq \varepsilon_{i,m}$ with $\varepsilon_{i,m} > 0$.

According to Lemma 3, one can obtain

$$\frac{z_{i,m}}{h_{i,m}} \varphi_{i,m} \leq \frac{|z_{i,m}|}{h_{i,m}} (\|W_{i,m}\| \|S_{i,m}\| + \varepsilon_{i,m}) \leq \frac{z_{i,m}^2}{2c_{i,m}^2 h_{i,m}^2} \|W_{i,m}\|^2 S_{i,m}^T S_{i,m} + \frac{1}{2} c_{i,m}^2 + \frac{z_{i,m}^2}{2h_{i,m}^2} + \frac{1}{2} \varepsilon_{i,m}^2 \tag{39}$$

where $c_{i,m}$ is a positive parameter to be designed.

Substituting (39) into (37), the following inequality holds

$$\begin{aligned}
\dot{V}_{i,m} &\leq -\sum_{j=1}^{m-1} g_{ij1} \frac{z_{i,j}^{\rho_1+1}}{h_{i,j}^{\frac{\rho_1+1}{2}}} - \sum_{j=1}^{m-1} g_{ij2} \frac{z_{i,j}^{\rho_2+1}}{h_{i,j}^{\frac{\rho_2+1}{2}}} + \sum_{j=1}^{m-1} \frac{z_{i,j}^2}{2c_{i,j}^2 h_{i,j}^2} (\|W_{i,j}\|^2 - \hat{\theta}_i) S_{i,j}^T S_{i,j} + \sum_{j=1}^{m-1} K_{i,j} + \frac{1}{2} \sum_{j=1}^m (c_{i,j}^2 + \varepsilon_{i,j}^2 + \bar{\omega}_{i,j}^2) \\
&\quad + \frac{z_{i,m}^2}{h_{i,m}^2} + \frac{z_{i,m}}{h_{i,m}} x_{i,m+1} + \frac{z_{i,m}^2}{2c_{i,m}^2 h_{i,m}^2} \|W_{i,m}\|^2 S_{i,m}^T S_{i,m} + \frac{\dot{k}_{i,m}}{k_{i,m}} - \frac{k_{i,m}\dot{k}_{i,m}}{h_{i,m}}
\end{aligned} \tag{40}$$

Construct the virtual control law $\alpha_{i,m}$ as

$$\alpha_{i,m} = -g_{im1} \frac{z_{i,m}^{\rho_1}}{h_{i,m}^{\frac{\rho_1-1}{2}}} - g_{im2} \frac{z_{i,m}^{\rho_2}}{h_{i,m}^{\frac{\rho_2-1}{2}}} - \frac{2z_{i,m}}{h_{i,m}} - \dot{k}_{i,m} - \frac{z_{i,m}}{2c_{i,m}^2 h_{i,m}} \hat{\theta}_i S_{i,m}^T S_{i,m} \tag{41}$$

where $g_{im1} > 0$, $g_{im2} > 0$ are parameters to be designed.

Substituting (41) into (40) yields

$$\begin{aligned}
\dot{V}_{i,m} &\leq -\sum_{j=1}^m g_{ij1} \frac{z_{i,j}^{\rho_1+1}}{h_{i,j}^{\frac{\rho_1+1}{2}}} - \sum_{j=1}^m g_{ij2} \frac{z_{i,j}^{\rho_2+1}}{h_{i,j}^{\frac{\rho_2+1}{2}}} + \sum_{j=1}^m \frac{z_{i,j}^2}{2c_{i,j}^2 h_{i,j}^2} (\|W_{i,j}\|^2 - \hat{\theta}_i) S_{i,j}^T S_{i,j} + \sum_{j=1}^{m-1} K_{i,j} + \frac{1}{2} \sum_{j=1}^m (c_{i,j}^2 + \varepsilon_{i,j}^2 + \bar{\omega}_{i,j}^2) \\
&\quad - \frac{z_{i,m}^2}{h_{i,m}^2} + \frac{z_{i,m}}{h_{i,m}} (x_{i,m+1} - \alpha_{i,m}) + \frac{z_{i,m}}{h_{i,m}} \left(-\dot{k}_{i,m} - \frac{k_{i,m}\dot{k}_{i,m}}{z_{i,m}} \right) + \frac{\dot{k}_{i,m}}{k_{i,m}}
\end{aligned} \tag{42}$$

Similar to (29) and (30), the following inequalities hold

$$\frac{z_{i,m}}{h_{i,m}} \left(-\dot{k}_{i,m} - \frac{k_{i,m} \dot{k}_{i,m}}{z_{i,m}} \right) \leq \frac{z_{i,m}^2}{h_{i,m}^2} + (\dot{k}_{i,m})^2 \quad (43)$$

$$\frac{\dot{k}_{i,m}}{k_{i,m}} + (\dot{k}_{i,m})^2 \leq K_{i,m} \quad (44)$$

Substituting (43)-(44) into (42), we have

$$\begin{aligned} \dot{V}_{i,m} \leq & - \sum_{j=1}^m g_{ij1} \frac{z_{i,j}^{\rho_1+1}}{h_{i,j}^{\frac{\rho_1+1}{2}}} - \sum_{j=1}^m g_{ij2} \frac{z_{i,j}^{\rho_2+1}}{h_{i,j}^{\frac{\rho_2+1}{2}}} + \sum_{j=1}^m \frac{z_{i,j}^2}{2c_{i,j}^2 h_{i,j}^2} (\|W_{i,j}\|^2 - \hat{\theta}_i) S_{i,j}^T S_{i,j} + \frac{z_{i,m}}{h_{i,m}} (x_{i,m+1} - \alpha_{i,m}) \\ & + \sum_{j=1}^m K_{i,j} + \frac{1}{2} \sum_{j=1}^m (c_{i,j}^2 + \varepsilon_{i,j}^2 + \bar{\omega}_{i,j}^2) \end{aligned} \quad (45)$$

Step i, n_i : Consider the tracking error $z_{i,n_i} = x_{i,n_i} - \alpha_{i,n_i-1}$, its time derivative is

$$\dot{z}_{i,n_i} = \dot{x}_{i,n_i} - \dot{\alpha}_{i,n_i-1} = u_i + f_{i,n_i} + \omega_{i,n_i} - \dot{\alpha}_{i,n_i-1} \quad (46)$$

Define the time-varying function $k_{i,n_i}(t)$ as

$$k_{i,n_i}(t) = (k_{n_i,a} - k_{n_i,b})e^{-l_{n_i}t} + k_{n_i,b} \quad (47)$$

where constants $k_{n_i,a} > k_{n_i,b} > 0$ and $l_{n_i} > 0$. Obviously, the time-varying function $k_{i,n_i}(t)$ is positive bounded and differentiable and $k_{n_i,b} < k_{i,n_i}(t) < k_{n_i,a}$ holds.

Choose the following Barrier Lyapunov function as

$$V_{i,n_i} = V_{i,n_i-1} + \frac{1}{2} \log \frac{k_{i,n_i}^2(t)}{h_{i,n_i}} + \frac{1}{2} \tilde{\theta}_i^2 \quad (48)$$

where $h_{i,n_i} = k_{i,n_i}^2(t) - z_{i,n_i}^2$.

The time derivative of V_{i,n_i} is obtained as

$$\dot{V}_{i,n_i} = \dot{V}_{i,n_i-1} + \frac{z_{i,n_i}}{h_{i,n_i}} (u_i + f_{i,n_i} + \omega_{i,n_i} - \dot{\alpha}_{i,n_i-1}) + \frac{\dot{k}_{i,n_i}}{k_{i,n_i}} - \frac{k_{i,n_i} \dot{k}_{i,n_i}}{h_{i,n_i}} - \tilde{\theta}_i \hat{\theta}_i \quad (49)$$

According to Lemma 3, one has

$$\frac{z_{i,n_i}}{h_{i,n_i}} \omega_{i,n_i} \leq \frac{z_{i,n_i}^2}{2h_{i,n_i}^2} + \frac{1}{2} \bar{\omega}_{i,n_i}^2 \quad (50)$$

Substituting (50) into (49), one has

$$\begin{aligned} \dot{V}_{i,n_i} \leq & - \sum_{j=1}^{n_i-1} g_{ij1} \frac{z_{i,j}^{\rho_1+1}}{h_{i,j}^{\frac{\rho_1+1}{2}}} - \sum_{j=1}^{n_i-1} g_{ij2} \frac{z_{i,j}^{\rho_2+1}}{h_{i,j}^{\frac{\rho_2+1}{2}}} + \sum_{j=1}^{n_i-1} \frac{z_{i,j}^2}{2c_{i,j}^2 h_{i,j}^2} (\|W_{i,j}\|^2 - \hat{\theta}_i) S_{i,j}^T S_{i,j} + \frac{z_{i,n_i-1}}{h_{i,n_i-1}} (x_{i,n_i} - \alpha_{i,n_i-1}) + \frac{1}{2} \sum_{j=1}^{n_i-1} (c_{i,j}^2 + \varepsilon_{i,j}^2 + \bar{\omega}_{i,j}^2) \\ & + \sum_{j=1}^{n_i-1} K_{i,j} + \frac{z_{i,n_i}}{h_{i,n_i}} (f_{i,n_i} + u_i - \dot{\alpha}_{i,n_i-1}) + \frac{z_{i,n_i}^2}{2h_{i,n_i}^2} + \frac{1}{2} \bar{\omega}_{i,n_i}^2 + \frac{\dot{k}_{i,n_i}}{k_{i,n_i}} - \frac{k_{i,n_i} \dot{k}_{i,n_i}}{h_{i,n_i}} - \tilde{\theta}_i \hat{\theta}_i \\ = & - \sum_{j=1}^{n_i-1} g_{ij1} \frac{z_{i,j}^{\rho_1+1}}{h_{i,j}^{\frac{\rho_1+1}{2}}} - \sum_{j=1}^{n_i-1} g_{ij2} \frac{z_{i,j}^{\rho_2+1}}{h_{i,j}^{\frac{\rho_2+1}{2}}} + \sum_{j=1}^{n_i-1} \frac{z_{i,j}^2}{2c_{i,j}^2 h_{i,j}^2} (\|W_{i,j}\|^2 - \hat{\theta}_i) S_{i,j}^T S_{i,j} + \frac{1}{2} \sum_{j=1}^{n_i-1} (c_{i,j}^2 + \varepsilon_{i,j}^2 + \bar{\omega}_{i,j}^2) + \sum_{j=1}^{n_i-1} K_{i,j} \\ & + \frac{z_{i,n_i}}{h_{i,n_i}} (u_i + \varphi_{i,n_i}) + \frac{z_{i,n_i}^2}{2h_{i,n_i}^2} + \frac{1}{2} \bar{\omega}_{i,n_i}^2 + \frac{\dot{k}_{i,n_i}}{k_{i,n_i}} - \frac{k_{i,n_i} \dot{k}_{i,n_i}}{h_{i,n_i}} - \tilde{\theta}_i \hat{\theta}_i \end{aligned} \quad (51)$$

where $\varphi_{i,n_i} \triangleq \frac{z_{i,n_i-1} h_{i,n_i}}{h_{i,n_i-1}} + f_{i,n_i} - \dot{\alpha}_{i,n_i-1}$.

According to Lemma 7, φ_{i,n_i} can be approximated by RBF NNs as

$$\varphi_{i,n_i} = W_{i,n_i}^T S_{i,n_i} + \Delta_{i,n_i} \quad (52)$$

where Δ_{i,n_i} is the approximation error satisfying $|\Delta_{i,n_i}| \leq \varepsilon_{i,n_i}$ with $\varepsilon_{i,n_i} > 0$.

According to Lemma 3, one can obtain

$$\frac{z_{i,n_i}}{h_{i,n_i}} \varphi_{i,n_i} \leq \frac{|z_{i,n_i}|}{h_{i,n_i}} (\|W_{i,n_i}\| \|S_{i,n_i}\| + \varepsilon_{i,n_i}) \leq \frac{z_{i,n_i}^2}{2c_{i,n_i}^2 h_{i,n_i}^2} \|W_{i,n_i}\|^2 S_{i,n_i}^T S_{i,n_i} + \frac{1}{2} c_{i,n_i}^2 + \frac{z_{i,n_i}^2}{2h_{i,n_i}^2} + \frac{1}{2} \varepsilon_{i,n_i}^2 \quad (53)$$

where c_{i,n_i} is a positive parameter to be designed.

Substituting (53) into (51), the following inequality holds

$$\begin{aligned} \dot{V}_{i,n_i} \leq & - \sum_{j=1}^{n_i-1} g_{ij1} \frac{z_{i,j}^{\rho_1+1}}{h_{i,j}^{\frac{\rho_1+1}{2}}} - \sum_{j=1}^{n_i-1} g_{ij2} \frac{z_{i,j}^{\rho_2+1}}{h_{i,j}^{\frac{\rho_2+1}{2}}} + \sum_{j=1}^{n_i-1} \frac{z_{i,j}^2}{2c_{i,j}^2 h_{i,j}^2} (\|W_{i,j}\|^2 - \hat{\theta}_i) S_{i,j}^T S_{i,j} + \frac{1}{2} \sum_{j=1}^{n_i} (c_{i,j}^2 + \varepsilon_{i,j}^2 + \bar{\omega}_{i,j}^2) \\ & + \sum_{j=1}^{n_i-1} K_{i,j} + \frac{z_{i,n_i}^2}{2c_{i,n_i}^2 h_{i,n_i}^2} \|W_{i,n_i}\|^2 S_{i,n_i}^T S_{i,n_i} + \frac{z_{i,n_i}}{h_{i,n_i}} u_i + \frac{z_{i,n_i}^2}{h_{i,n_i}^2} + \frac{\dot{k}_{i,n_i}}{k_{i,n_i}} - \frac{k_{i,n_i} \dot{k}_{i,n_i}}{h_{i,n_i}} - \tilde{\theta}_i \hat{\theta}_i \end{aligned} \quad (54)$$

Construct the virtual control law α_{i,n_i} as

$$\alpha_{i,n_i} = -g_{in_1} \frac{z_{i,n_i}^{\rho_1}}{h_{i,n_i}^{\frac{\rho_1-1}{2}}} - g_{in_2} \frac{z_{i,n_i}^{\rho_2}}{h_{i,n_i}^{\frac{\rho_2-1}{2}}} - \frac{2z_{i,n_i}}{h_{i,n_i}} - \dot{k}_{i,n_i} - \frac{z_{i,n_i}}{2c_{i,n_i}^2 h_{i,n_i}} \hat{\theta}_i S_{i,n_i}^T S_{i,n_i} \quad (55)$$

Substituting (55) into (54) yields

$$\begin{aligned} \dot{V}_{i,n_i} \leq & - \sum_{j=1}^{n_i} g_{ij1} \frac{z_{i,j}^{\rho_1+1}}{h_{i,j}^{\frac{\rho_1+1}{2}}} - \sum_{j=1}^{n_i} g_{ij2} \frac{z_{i,j}^{\rho_2+1}}{h_{i,j}^{\frac{\rho_2+1}{2}}} + \sum_{j=1}^{n_i} \frac{z_{i,j}^2}{2c_{i,j}^2 h_{i,j}^2} (\|W_{i,j}\|^2 - \hat{\theta}_i) S_{i,j}^T S_{i,j} + \frac{z_{i,n_i}}{h_{i,n_i}} (u_i - \alpha_{i,n_i}) \\ & - \frac{z_{i,n_i}^2}{h_{i,n_i}^2} + \frac{z_{i,n_i}}{h_{i,n_i}} \left(-\dot{k}_{i,n_i} - \frac{k_{i,n_i} \dot{k}_{i,n_i}}{z_{i,n_i}} \right) + \frac{\dot{k}_{i,n_i}}{k_{i,n_i}} - \tilde{\theta}_i \hat{\theta}_i + \frac{1}{2} \sum_{j=1}^{n_i} (c_{i,j}^2 + \varepsilon_{i,j}^2 + \bar{\omega}_{i,j}^2) + \sum_{j=1}^{n_i-1} K_{i,j} \end{aligned} \quad (56)$$

Similar to (29)-(30) and (43)-(44), the following inequalities can be obtained

$$\frac{z_{i,n_i}}{h_{i,n_i}} \left(-\dot{k}_{i,n_i} - \frac{k_{i,n_i} \dot{k}_{i,n_i}}{z_{i,n_i}} \right) \leq \frac{z_{i,n_i}^2}{h_{i,n_i}^2} + (\dot{k}_{i,n_i})^2 \quad (57)$$

$$\frac{\dot{k}_{i,n_i}}{k_{i,n_i}} + (\dot{k}_{i,n_i})^2 \leq K_{i,n_i} \quad (58)$$

Substituting (57)-(58) into (56), it has

$$\begin{aligned} \dot{V}_{i,n_i} \leq & - \sum_{j=1}^{n_i} g_{ij1} \frac{z_{i,j}^{\rho_1+1}}{h_{i,j}^{\frac{\rho_1+1}{2}}} - \sum_{j=1}^{n_i} g_{ij2} \frac{z_{i,j}^{\rho_2+1}}{h_{i,j}^{\frac{\rho_2+1}{2}}} + \sum_{j=1}^{n_i} \frac{z_{i,j}^2}{2c_{i,j}^2 h_{i,j}^2} (\|W_{i,j}\|^2 - \hat{\theta}_i) S_{i,j}^T S_{i,j} + \frac{z_{i,n_i}}{h_{i,n_i}} (u_i - \alpha_{i,n_i}) \\ & - \tilde{\theta}_i \hat{\theta}_i + \frac{1}{2} \sum_{j=1}^{n_i} (c_{i,j}^2 + \varepsilon_{i,j}^2 + \bar{\omega}_{i,j}^2) + \sum_{j=1}^{n_i} K_{i,j} \end{aligned} \quad (59)$$

Construct the parameter updating law $\hat{\theta}_i$ as

$$\dot{\hat{\theta}}_i = -\lambda_i \hat{\theta}_i + \sum_{j=1}^{n_i} \frac{z_{i,j}^2}{2c_{i,j}^2 h_{i,j}^2} S_{i,j}^T S_{i,j} \quad (60)$$

where λ_i is a positive parameter to be designed.

According to the definition of θ_i and Lemma 3, we have the following inequality

$$\begin{aligned} \sum_{j=1}^{n_i} \frac{z_{i,j}^2}{2c_{i,j}^2 h_{i,j}^2} (\|W_{i,j}\|^2 - \hat{\theta}_i) S_{i,j}^T S_{i,j} - \tilde{\theta}_i \hat{\theta}_i &= \sum_{j=1}^{n_i} \frac{z_{i,j}^2}{2c_{i,j}^2 h_{i,j}^2} (\|W_{i,j}\|^2 - \hat{\theta}_i) S_{i,j}^T S_{i,j} - \sum_{j=1}^{n_i} \frac{z_{i,j}^2}{2c_{i,j}^2 h_{i,j}^2} \tilde{\theta}_i S_{i,j}^T S_{i,j} + \lambda_i \tilde{\theta}_i \hat{\theta}_i \\ &\leq \lambda_i \tilde{\theta}_i \hat{\theta}_i \end{aligned} \quad (61)$$

Substituting (61) into (59), one can obtain

$$\dot{V}_{i,n_i} \leq - \sum_{j=1}^{n_i} g_{ij1} \frac{z_{i,j}^{\rho_1+1}}{h_{i,j}^{\frac{\rho_1+1}{2}}} - \sum_{j=1}^{n_i} g_{ij2} \frac{z_{i,j}^{\rho_2+1}}{h_{i,j}^{\frac{\rho_2+1}{2}}} + \frac{z_{i,n_i}}{h_{i,n_i}} (u_i - \alpha_{i,n_i}) + \lambda_i \tilde{\theta}_i \hat{\theta}_i + \frac{1}{2} \sum_{j=1}^{n_i} (c_{i,j}^2 + \varepsilon_{i,j}^2 + \bar{\omega}_{i,j}^2) + \sum_{j=1}^{n_i} K_{i,j} \quad (62)$$

According to the ETM, $u_i(t) = \Psi_i(t_k)$ for $\forall t \in [t_k, t_{k+1})$. Then, the controller is designed as

$$\Psi_i(t) = -(1 + \gamma_i) \left[\alpha_{i,n_i} \tanh \left(\frac{z_{i,n_i} \alpha_{i,n_i}}{\mu_i h_{i,n_i}} \right) + \bar{\eta}_i \tanh \left(\frac{\bar{\eta}_i z_{i,n_i}}{\mu_i h_{i,n_i}} \right) \right] \quad (63)$$

where $\bar{\eta}_i > \frac{\eta_i}{1-\gamma_i}$ and $\mu_i > 0$ are parameters to be designed.

By using actuator signal (15), controller (63) and Lemma 5, $\frac{z_{i,n_i}}{h_{i,n_i}} (u_i - \alpha_{i,n_i})$ in (62) follows

$$\begin{aligned} \frac{z_{i,n_i}}{h_{i,n_i}} (u_i - \alpha_{i,n_i}) &= M_i (u_i - \alpha_{i,n_i}) \\ &= M_i \left(\frac{\Psi_i(t)}{1 + \varsigma_1(t) \gamma_i} - \frac{\varsigma_2(t) \eta_i}{1 + \varsigma_1(t) \gamma_i} - \alpha_{i,n_i} \right) \\ &\leq \frac{M_i \Psi_i(t)}{1 + \varsigma_1(t) \gamma_i} + \frac{M_i \eta_i}{1 - \gamma_i} - M_i \alpha_{i,n_i} \\ &\leq -M_i \alpha_{i,n_i} \tanh \left(\frac{M_i \alpha_{i,n_i}}{\mu_i} \right) - M_i \bar{\eta}_i \tanh \left(\frac{M_i \bar{\eta}_i}{\mu_i} \right) + |M_i \bar{\eta}_i| + |M_i \alpha_{i,n_i}| \\ &\leq 0.557 \mu_i \end{aligned} \quad (64)$$

where $M_i = \frac{z_{i,n_i}}{h_{i,n_i}}$.

Substituting (64) into (62) yields

$$\dot{V}_{i,n_i} \leq - \sum_{j=1}^{n_i} g_{ij1} \frac{z_{i,j}^{\rho_1+1}}{h_{i,j}^{\frac{\rho_1+1}{2}}} - \sum_{j=1}^{n_i} g_{ij2} \frac{z_{i,j}^{\rho_2+1}}{h_{i,j}^{\frac{\rho_2+1}{2}}} + \lambda_i \tilde{\theta}_i \hat{\theta}_i + \frac{1}{2} \sum_{j=1}^{n_i} (c_{i,j}^2 + \varepsilon_{i,j}^2 + \bar{\omega}_{i,j}^2) + \sum_{j=1}^{n_i} K_{i,j} + 0.557 \mu_i \quad (65)$$

Remark 3. As can be seen from (19), (34) and (48), the Lyapunov function $V_{i,j}$ ($j = 1, 2, \dots, n_i$) is unbounded if $k_{i,j}(t) \leq |z_{i,j}|$ by adopting the BLF technique. Therefore, the tracking error $z_{i,j}$ will be confined to the predefined constraint region $|z_{i,j}| \leq k_{i,j}$ if the control scheme is designed effectively to ensure the boundedness of $V_{i,j}$. The coordinate transformation (16) has the following deformation

$$\begin{aligned} |x_{i,1}| &= |z_{i,1} + y_{i,d}| \leq |z_{i,1}| + |y_{i,d}| \leq k_{i,1} + |y_{i,d}|, j = 1 \\ |x_{i,j}| &= |z_{i,j} + \alpha_{i,j-1}| \leq |z_{i,j}| + |\alpha_{i,j-1}| \leq k_{i,j} + |\alpha_{i,j-1}|, j = 2, \dots, n_i \end{aligned} \quad (66)$$

Since $k_{i,j}$, $y_{i,d}$ and $\alpha_{i,j-1}$ are bounded, $|x_{i,j}|$ are bounded. Therefore, by choosing appropriate positive constant $\varkappa_{i,j}$, we have $|x_{i,j}| \leq k_{i,j} + \varkappa_{i,j} = \kappa_{i,j}$ ($j = 1, 2, \dots, n_i$), which guarantees that the system states fall in the time-varying constraints.

3.3 | Fixed time stability analysis

Choose the Lyapunov candidate function as

$$V_i(t) = V_{i,n_i}(t) \quad (67)$$

where $V_{i,n_i}(t)$ is defined in step i , n_i above.

Taking the time derivative of $V_i(t)$ yields

$$\dot{V}_i(t) = \dot{V}_{i,n_i}(t) \leq - \sum_{j=1}^{n_i} g_{ij1} \frac{z_{i,j}^{\rho_1+1}}{h_{i,j}^{\frac{\rho_1+1}{2}}} - \sum_{j=1}^{n_i} g_{ij2} \frac{z_{i,j}^{\rho_2+1}}{h_{i,j}^{\frac{\rho_2+1}{2}}} + \lambda_i \tilde{\theta}_i \hat{\theta}_i + \frac{1}{2} \sum_{j=1}^{n_i} (c_{i,j}^2 + \varepsilon_{i,j}^2 + \bar{\omega}_{i,j}^2) + \sum_{j=1}^{n_i} K_{i,j} + 0.557 \mu_i \quad (68)$$

According to Lemma 3, we have

$$\lambda_i \tilde{\theta}_i \hat{\theta}_i = \lambda_i (\theta_i - \hat{\theta}_i) \hat{\theta}_i = \lambda_i (\theta_i \hat{\theta}_i - \hat{\theta}_i^2) \leq \frac{1}{2} \lambda_i \theta_i^2 - \frac{1}{2} \lambda_i \tilde{\theta}_i^2 \quad (69)$$

Let $\alpha_1 = \frac{\rho_1+1}{2}$, $\alpha_2 = \frac{\rho_2+1}{2}$. According to Lemma 2, we have

$$-\frac{1}{2} \tilde{\theta}_i^2 + \left(\frac{1}{2} \tilde{\theta}_i^2\right)^{\alpha_1} \leq (1 - \alpha_1) \alpha_1^{\frac{\alpha_1}{1-\alpha_1}} \quad (70)$$

$$-\frac{1}{2} \tilde{\theta}_i^2 + \left(\frac{1}{2} \tilde{\theta}_i^2\right)^{\alpha_2} \leq (1 - \alpha_2) \alpha_2^{\frac{\alpha_2}{1-\alpha_2}} \quad (71)$$

From (70) and (71), we have the following inequality

$$-\tilde{\theta}_i^2 \leq -\left(\frac{1}{2} \tilde{\theta}_i^2\right)^{\alpha_1} - \left(\frac{1}{2} \tilde{\theta}_i^2\right)^{\alpha_2} + (1 - \alpha_1) \alpha_1^{\frac{\alpha_1}{1-\alpha_1}} \quad (72)$$

Substituting (69) and (72) into (68) yields

$$\begin{aligned} \dot{V}_i(t) &\leq - \sum_{j=1}^{n_i} g_{ij1} \left(\frac{z_{i,j}^2}{h_{i,j}}\right)^{\alpha_1} - \sum_{j=1}^{n_i} g_{ij2} \left(\frac{z_{i,j}^2}{h_{i,j}}\right)^{\alpha_2} - \frac{1}{2} \lambda_i \left(\frac{1}{2} \tilde{\theta}_i^2\right)^{\alpha_1} - \frac{1}{2} \lambda_i \left(\frac{1}{2} \tilde{\theta}_i^2\right)^{\alpha_2} + \frac{1}{2} \lambda (1 - \alpha_1) \alpha_1^{\frac{\alpha_1}{1-\alpha_1}} \\ &\quad + \frac{1}{2} \lambda_i \theta_i^2 + \frac{1}{2} \sum_{j=1}^{n_i} (c_{i,j}^2 + \varepsilon_{i,j}^2 + \bar{\omega}_{i,j}^2) + \sum_{j=1}^{n_i} K_{i,j} + 0.557 \mu_i \\ &\leq - r_1 \sum_{j=1}^{n_i} \left(\frac{z_{i,j}^2}{h_{i,j}}\right)^{\alpha_1} - r_2 \sum_{j=1}^{n_i} \left(\frac{z_{i,j}^2}{h_{i,j}}\right)^{\alpha_2} - \frac{1}{2} \lambda_i \left(\frac{1}{2} \tilde{\theta}_i^2\right)^{\alpha_1} - \frac{1}{2} \lambda_i \left(\frac{1}{2} \tilde{\theta}_i^2\right)^{\alpha_2} + \frac{1}{2} \sum_{j=1}^{n_i} (c_{i,j}^2 + \varepsilon_{i,j}^2 + \bar{\omega}_{i,j}^2) + \sum_{j=1}^{n_i} K_{i,j} + 0.557 \mu_i \end{aligned} \quad (73)$$

where $r_1 = \min \{g_{ij1}, j = 1, \dots, n_i\}$, $r_2 = \min \{g_{ij2}, j = 1, \dots, n_i\}$.

According to Lemma 4, we have

$$\begin{aligned} \dot{V}_i(t) &\leq - r_3 \left(\sum_{j=1}^{n_i} \frac{z_{i,j}^2}{h_{i,j}}\right)^{\alpha_1} - r_4 \left(\sum_{j=1}^{n_i} \frac{z_{i,j}^2}{h_{i,j}}\right)^{\alpha_2} - \frac{1}{2} \lambda_i \left(\frac{1}{2} \tilde{\theta}_i^2\right)^{\alpha_1} - \frac{1}{2} \lambda_i \left(\frac{1}{2} \tilde{\theta}_i^2\right)^{\alpha_2} + \frac{1}{2} \sum_{j=1}^{n_i} (c_{i,j}^2 + \varepsilon_{i,j}^2 + \bar{\omega}_{i,j}^2) + \sum_{j=1}^{n_i} K_{i,j} + 0.557 \mu_i \\ &\leq - r_5 \left(\sum_{j=1}^{n_i} \frac{1}{2} \log \frac{k_{i,j}^2(t)}{h_{i,j}}\right)^{\alpha_1} - r_6 \left(\sum_{j=1}^{n_i} \frac{1}{2} \log \frac{k_{i,j}^2(t)}{h_{i,j}}\right)^{\alpha_2} - \frac{1}{2} \lambda_i \left(\frac{1}{2} \tilde{\theta}_i^2\right)^{\alpha_1} - \frac{1}{2} \lambda_i \left(\frac{1}{2} \tilde{\theta}_i^2\right)^{\alpha_2} + \frac{1}{2} \sum_{j=1}^{n_i} (c_{i,j}^2 + \varepsilon_{i,j}^2 + \bar{\omega}_{i,j}^2) \\ &\quad + \sum_{j=1}^{n_i} K_{i,j} + 0.557 \mu_i \\ &\leq - P_i \left(\sum_{j=1}^{n_i} \frac{1}{2} \log \frac{k_{i,j}^2(t)}{h_{i,j}} + \frac{1}{2} \tilde{\theta}_i^2\right)^{\alpha_1} - Q_i \left(\sum_{j=1}^{n_i} \frac{1}{2} \log \frac{k_{i,j}^2(t)}{h_{i,j}} + \frac{1}{2} \tilde{\theta}_i^2\right)^{\alpha_2} + \frac{1}{2} \sum_{j=1}^{n_i} (c_{i,j}^2 + \varepsilon_{i,j}^2 + \bar{\omega}_{i,j}^2) + \sum_{j=1}^{n_i} K_{i,j} + 0.557 \mu_i \\ &= - P_i V_i^{\alpha_1}(t) - Q_i V_i^{\alpha_2}(t) + \beta_i \end{aligned} \quad (74)$$

where $r_3 = r_1$, $r_4 = n_i^{1-\alpha_2} r_2$, $r_5 = 2^{\alpha_1} r_3$, $r_6 = 2^{\alpha_2} r_4$, $P_i = \min \{r_5, \frac{1}{2} \lambda_i\}$, $Q_i = 2^{1-\alpha_2} \min \{r_6, \frac{1}{2} \lambda_i\}$, $\beta_i = \frac{1}{2} \sum_{j=1}^{n_i} (c_{i,j}^2 + \varepsilon_{i,j}^2 + \bar{\omega}_{i,j}^2) + \sum_{j=1}^{n_i} K_{i,j} + 0.557 \mu_i$.

According to Lemma 1, it is known that all the signals of system are semiglobal practical fixed time stable and converge to the following reside set within the time T_f

$$\Omega = \left\{ x \mid V(x) \leq \min \left\{ \left(\frac{\beta_i}{P_i(1-t)}\right)^{\frac{1}{\alpha_1}}, \left(\frac{\beta_i}{Q_i(1-t)}\right)^{\frac{1}{\alpha_2}} \right\} \right\}$$

and the time T_f is bounded by T_{\max}

$$T_f \leq T_{\max} := \frac{1}{P_i \iota (1 - \alpha_1)} + \frac{1}{Q_i \iota (\alpha_2 - 1)} \quad (75)$$

with $0 < \iota < 1$ is a positive parameter.

Next, we will prove that the Zeno phenomenon does not occur in the designed controller.

Obviously, the controller $\Psi_i(t)$ in (63) is continuous, the error signal $e_i(t) = \psi_i(t) - \Psi_i(t_k)$ is also continuous. As $\Psi_i(t_k)$ is a constant for $\forall t \in [t_k, t_{k+1})$, $\dot{e}_i(t) = \dot{\Psi}_i(t)$ for $\forall t \in [t_k, t_{k+1})$. Moreover, it is easy to verify that $\dot{\Psi}_i(t)$ is continuous, so there exists an upper bound $D > 0$ such that

$$|\dot{\psi}_i(t)| \leq D \quad \forall t \in [t_k, t_{k+1}) \quad (76)$$

From the event-triggered theory, one has that $e_i(t_k) = 0$ and $|e_i(t_{k+1}^-)| = \gamma |\psi_i(t_k)| + \eta_i \geq \eta_i$. And then we have the following inequality

$$|\dot{e}_i(t_k)| = \frac{|e_i(t_{k+1}^-) - e_i(t_k)|}{t_{k+1} - t_k} \leq D \quad (77)$$

From (77), we can obtain $t_{k+1} - t_k \geq \frac{|e_i(t_{k+1}^-) - e_i(t_k)|}{D} \geq \frac{\eta_i}{D}$. Define $t_{\min} \triangleq \frac{\eta_i}{D}$, hence the Zeno behaviour is effectively avoided, i.e., $t_{k+1} - t_k \geq t_{\min}$.

4 | SIMULATION RESULTS

In this section, two representative examples will be given to illustrate the proposed control scheme.

4.1 | Example 1

Consider the following third-order nonlinear system, which contains two subsystems

$$\begin{cases} \dot{x}_{i,1}(t) = x_{i,2}(t) + f_{i,1} + \omega_{i,1}(t), \\ \dot{x}_{i,2}(t) = x_{i,3}(t) + f_{i,2} + \omega_{i,2}(t), \\ \dot{x}_{i,3}(t) = u_i(t) + f_{i,3} + \omega_{i,3}(t), \\ y_i(t) = x_{i,1}(t), i = 1, 2 \end{cases} \quad (78)$$

where $f_{1,1} = 0.5 \sin(x_{1,1})$, $f_{1,2} = x_{1,2} \cos(x_{1,2})$, $f_{1,3} = 2x_{1,2} \sin(x_{1,3})$, $f_{2,1} = 0.3 \sin(x_{2,1})$, $f_{2,2} = x_{2,2} \sin(x_{2,2})$, $f_{2,3} = 2x_{2,3} \cos(x_{2,2})$, The external disturbances $\omega_{i,j}(t)$ ($j = 1, 2, 3$) are the Gaussian white noise with zero mean and 0.005 standard deviation. The reference signals are: $y_{1,d} = 0.4 \sin(0.5t) + 1.5 \sin(t)$, $y_{2,d} = 0.5 \sin(t) + 1.6 \cos(0.5t)$. The initial values of $[x_{1,1}, x_{1,2}, x_{1,3}]^T$ are set as $[0.5, 0.5, -10.5]^T$. The initial values of $[x_{2,1}, x_{2,2}, x_{2,3}]^T$ are set as $[0.5, 5.5, 8.5]^T$. The initial values of $[z_{1,1}, z_{1,2}, z_{1,3}]^T$ are set as $[0.5, 0.5, 0.5]^T$. The initial values of $[z_{2,1}, z_{2,2}, z_{2,3}]^T$ are set as $[0.5, 0.5, 0.5]^T$. The error $z_{i,j}$ are limited by $|z_{i,j}| < k_{i,j}$, ($i = 1, 2; j = 1, 2, 3$). To guarantee favorable performances, we choose $k_{1,1} = 2e^{-2t} + 0.7$, $k_{1,2} = 6e^{-t} + 0.5$, $k_{1,3} = 32e^{-t} + 5$, $k_{2,1} = 2e^{-2t} + 0.7$, $k_{2,2} = 6e^{-t} + 0.5$, $k_{2,3} = 32e^{-t} + 5$ in this simulation.

The Gaussian basic function of NNs are chosen as

$$\begin{aligned} s_{G_{i,j}^1}(z_{i,j}) &= \exp\left[-\frac{(z_{i,j} - 1)^2}{0.5}\right], s_{G_{i,j}^2}(z_{i,j}) = \exp\left[-\frac{(z_{i,j} - 0.5)^2}{0.5}\right], s_{G_{i,j}^3}(z_{i,j}) = \exp\left[-\frac{(z_{i,j} - 0)^2}{0.5}\right], \\ s_{G_{i,j}^4}(z_{i,j}) &= \exp\left[-\frac{(z_{i,j} + 0.5)^2}{0.5}\right], s_{G_{i,j}^5}(z_{i,j}) = \exp\left[-\frac{(z_{i,j} + 1)^2}{0.5}\right] \end{aligned}$$

The virtual control laws and the adaptive law are constructed as

$$\begin{aligned}\alpha_{i,1} &= -g_{i11} \frac{z_{i,1}^{\rho_1}}{h_{i,1}^{\frac{\rho_1-1}{2}}} - g_{i12} \frac{z_{i,1}^{\rho_2}}{h_{i,1}^{\frac{\rho_2-1}{2}}} - \frac{2z_{i,1}}{h_{i,1}} - \dot{k}_{i,1} + \dot{y}_{i,d} - \frac{z_{i,1}}{2c_{i,1}^2 h_{i,1}} \hat{\theta}_i S_{i,1}^T S_{i,1} \\ \alpha_{i,2} &= -g_{i21} \frac{z_{i,2}^{\rho_1}}{h_{i,2}^{\frac{\rho_1-1}{2}}} - g_{i22} \frac{z_{i,2}^{\rho_2}}{h_{i,2}^{\frac{\rho_2-1}{2}}} - \frac{2z_{i,2}}{h_{i,2}} - \dot{k}_{i,2} - \frac{z_{i,2}}{2c_{i,2}^2 h_{i,2}} \hat{\theta}_i S_{i,2}^T S_{i,2} \\ \alpha_{i,3} &= -g_{i31} \frac{z_{i,3}^{\rho_1}}{h_{i,3}^{\frac{\rho_1-1}{2}}} - g_{i32} \frac{z_{i,3}^{\rho_2}}{h_{i,3}^{\frac{\rho_2-1}{2}}} - \frac{2z_{i,3}}{h_{i,3}} - \dot{k}_{i,3} - \frac{z_{i,3}}{2c_{i,3}^2 h_{i,3}} \hat{\theta}_i S_{i,3}^T S_{i,3}\end{aligned}\quad (79)$$

$$\hat{\theta}_i = -\lambda_i \hat{\theta}_i + \sum_{j=1}^3 \frac{z_{i,j}^2}{2c_{i,j}^2 h_{i,j}^2} S_{i,j}^T S_{i,j} \quad (80)$$

The parameters of the above equations are given as $g_{111} = g_{112} = 4$, $g_{121} = g_{122} = 6$, $g_{131} = g_{132} = 9$, $g_{211} = g_{212} = 3$, $g_{221} = g_{222} = 4$, $g_{231} = g_{232} = 20$, $c_{1,1} = c_{1,2} = c_{2,1} = c_{2,2} = 1$, $\lambda_1 = 3$, $\lambda_2 = 1$, $\rho_1 = \frac{9}{11}$, $\rho_2 = \frac{11}{9}$, $\gamma_1 = \gamma_2 = 0.8$, $\eta_1 = \eta_2 = 1$, $\bar{\eta}_1 = \bar{\eta}_2 = 5.01$, $\mu_1 = \mu_2 = 0.2$.

The controller is designed as

$$\Psi_i(t) = -1.8 \left[\alpha_{i,3} \tanh \left(\frac{z_{i,3} \alpha_{i,3}}{0.2 h_{i,3}} \right) + 5.01 \tanh \left(\frac{5.01 z_{i,3}}{0.2 h_{i,3}} \right) \right] \quad (81)$$

The triggering condition is defined by

$$\begin{aligned}u_i(t) &= \Psi_i(t_k) \quad \forall t \in [t_k, t_{k+1}) \\ t_{k+1} &= \inf \{ t > t_k \mid |e_i(t)| \geq 0.8 |\Psi_i(t_k)| + 1 \}\end{aligned}\quad (82)$$

The simulation results are shown in Fig. 1-6. Fig. 2 shows the system reference signals $y_{1,d}$, $y_{2,d}$ of two subsystems and the output of the system with different initial values, respectively. It can be seen intuitively from the figure that the two subsystems can track the reference signal in a fixed time under different initial conditions, which verifies the superiority of fixed-time stability.

Then, Figure. 3 - 6 shows the simulation results of two subsystems when the initial condition is $x_{1,1}(0) = x_{2,1}(0) = 0.5$. Fig. 3 (a), (c), (e) show the states of subsystem 1, Fig. 3 (b), (d), (f) show the states of subsystem 2. It is clear that all states of both subsystems are constrained within bounds. Form Fig 5, we can see that the tracking error of the system are also constrained within the given range. Therefore, both the state and tracking error of the system can be constrained within a predefined time-varying function. The control signal $\psi(t)$ and output signal $u(t)$ of two subsystems are given in Fig 4. Obviously, the actuator is a constant between two triggering intervals, which clearly shows the characteristics of event-triggered scheme.

Fig. 6 depicts the inter-event execution intervals of two subsystems. The abscissa represents the instant of event triggering and the height represents the time between two triggering events. The higher the ordinate is, the longer the interval between two adjacent event triggering instant is. The system sampling time is 0.01s. It can be clearly observed from Fig. 6 that most triggering intervals are longer than 0.01s, which shows that the event-triggering mechanism has less triggering time than the time-triggering mechanism and saves more network resources.

The advantages of the fixed time control strategy over the finite time control strategy are further shown in Fig. 7, where the finite time control strategy in literature [15] is applied to system (78) and the system control parameters and RBF NNs are selected the same as the above cases. Fig. 7 (a) describes the system output of the proposed fixed-time control scheme and the finite-time control in literature [15]. Fig. 7 (b) shows the tracking error of the two control schemes. It can be seen that the fixed time strategy mentioned above not only has faster convergence rate and better tracking performance than the finite time strategy, but also has smaller tracking error.

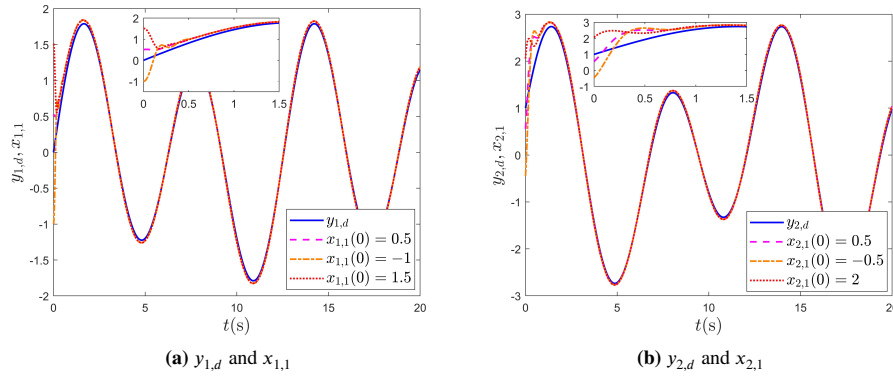
The superiority of event-triggered strategy in saving network resources is shown in Table 1. The sampling time interval is 0.01s, and the simulation duration is 20s.

It can be seen intuitively from Table 1 that the number of triggering events (NET) of subsystems 1 and 2 is significantly reduced than that of literature [15]. Meanwhile, the transmission percentage of the two subsystems is less than 50%, while that of

TABLE 1 Number of triggering events (NTE) and transmission percentage

	Sampling times	NET	Percentage
Sub1	2000	873	43.65%
Sub2	2000	568	28.4%
literature [15]	2000	2000	100%

literature [15] is 100%. These can well prove that the introduction of event-triggered strategy can save communication resources and improve communication efficiency.

**FIGURE 2** System reference signal and output y

4.2 | Example 2

To further illustrate the effectiveness of the proposed method in practical applications, vehicle platoon system is taken as another example in the simulation study. Consider a vehicle platoon system consisting of one leader and three following vehicles depicted in Fig. 8, where L represents the length of the vehicles and d represents the distance between consecutive vehicles.

The vehicle dynamic model can be described as[35]

$$\begin{cases} \dot{x}_i = v_i \\ \dot{v}_i = a_i \\ \dot{a}_i = -\frac{1}{\zeta_i} \left(\dot{v}_i + \frac{\sigma A_i C_{d_i}}{2m_i} v_i^2 + \frac{d_{m_i}}{m_i} \right) - \frac{\sigma A_i C_{d_i} v_i a_i}{m_i} + \frac{1}{\zeta_i m_i} u_i, 1 \leq i \leq 3 \end{cases} \quad (83)$$

where x_i , v_i , a_i represent the position, velocity and acceleration of the i th vehicle, respectively. u_i is the control input of the i th vehicle's engine, with $u_i > 0$ representing the throttle input and $u_i < 0$ representing the brake input. σ represents the specific mass of the air. For the i th vehicle, ζ_i is the engine's time constant, m_i is the vehicle mass, A_i represents the cross-sectional area, C_{d_i} depicts the drag coefficient, $\frac{\sigma A_i C_{d_i}}{2m_i}$ is the air resistance, d_{m_i} displays the mechanical drag.

Parameters of the vehicle are set as: $\sigma=1.2\text{kg/m}^3$, $\zeta_i = 0.25$, $m_i=1464\text{kg}$, $A_i=2.2\text{m}^2$, $C_{d_i}=0.35$, $d_{m_i}=5\text{N}$. For the constraint term, we choose $k_{1,1} = k_{2,1} = k_{3,1} = 2e^{-2t} + 0.7$, $k_{1,2} = k_{2,2} = k_{3,2} = 2e^{-2t} + 0.5$, $k_{1,3} = k_{2,3} = k_{3,3} = 32e^{-t} + 5$.

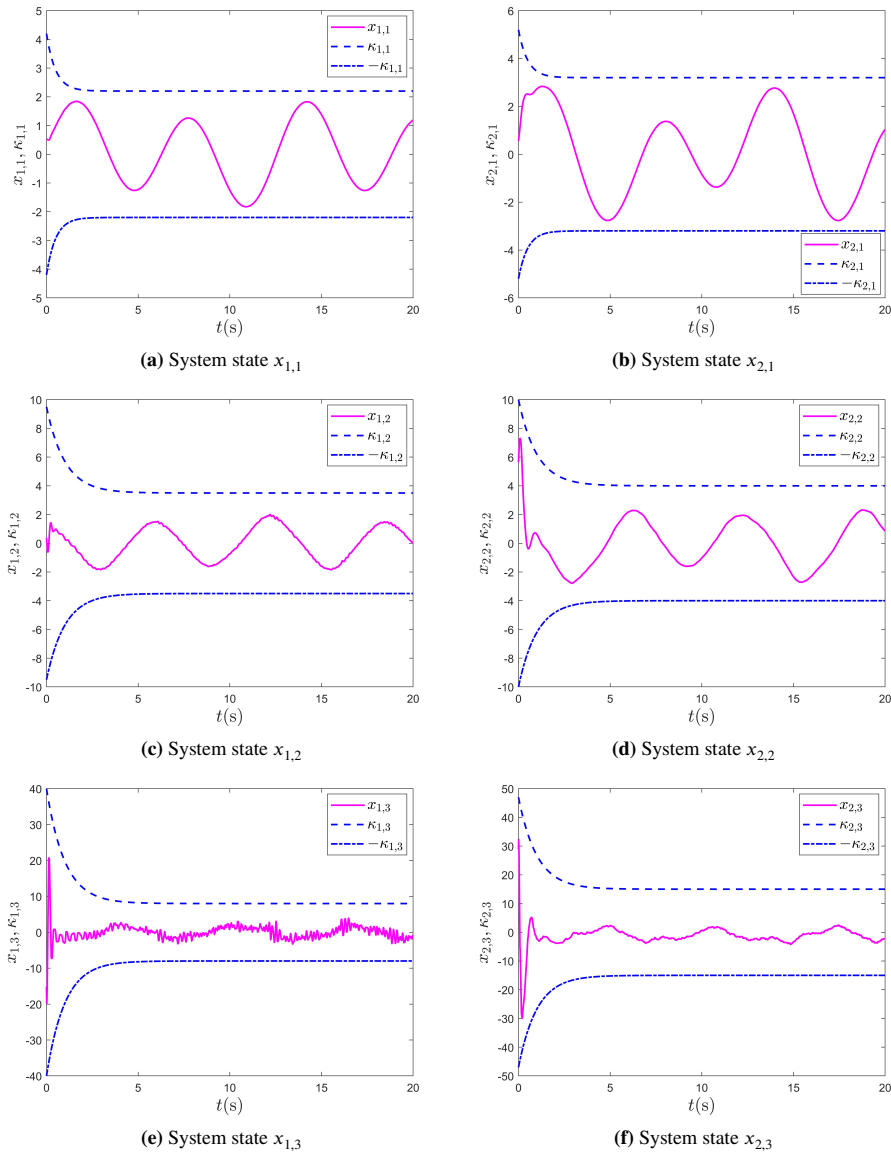


FIGURE 3 System states $x_{i,j}$ ($i = 1, 2$ $j = 1, 2, 3$)

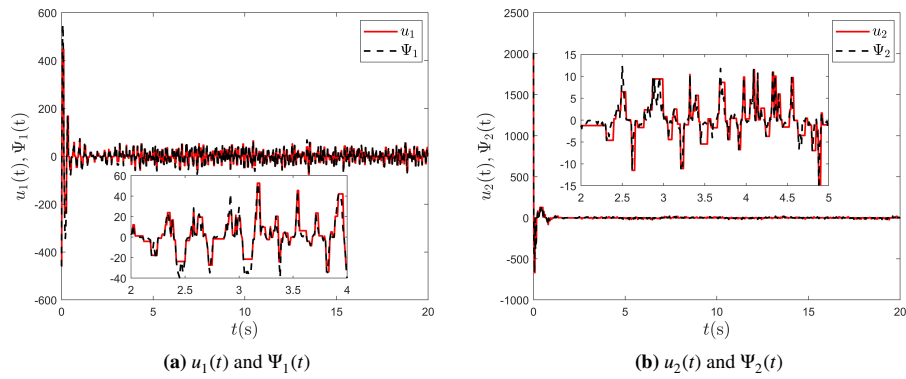


FIGURE 4 Control input of two subsystems

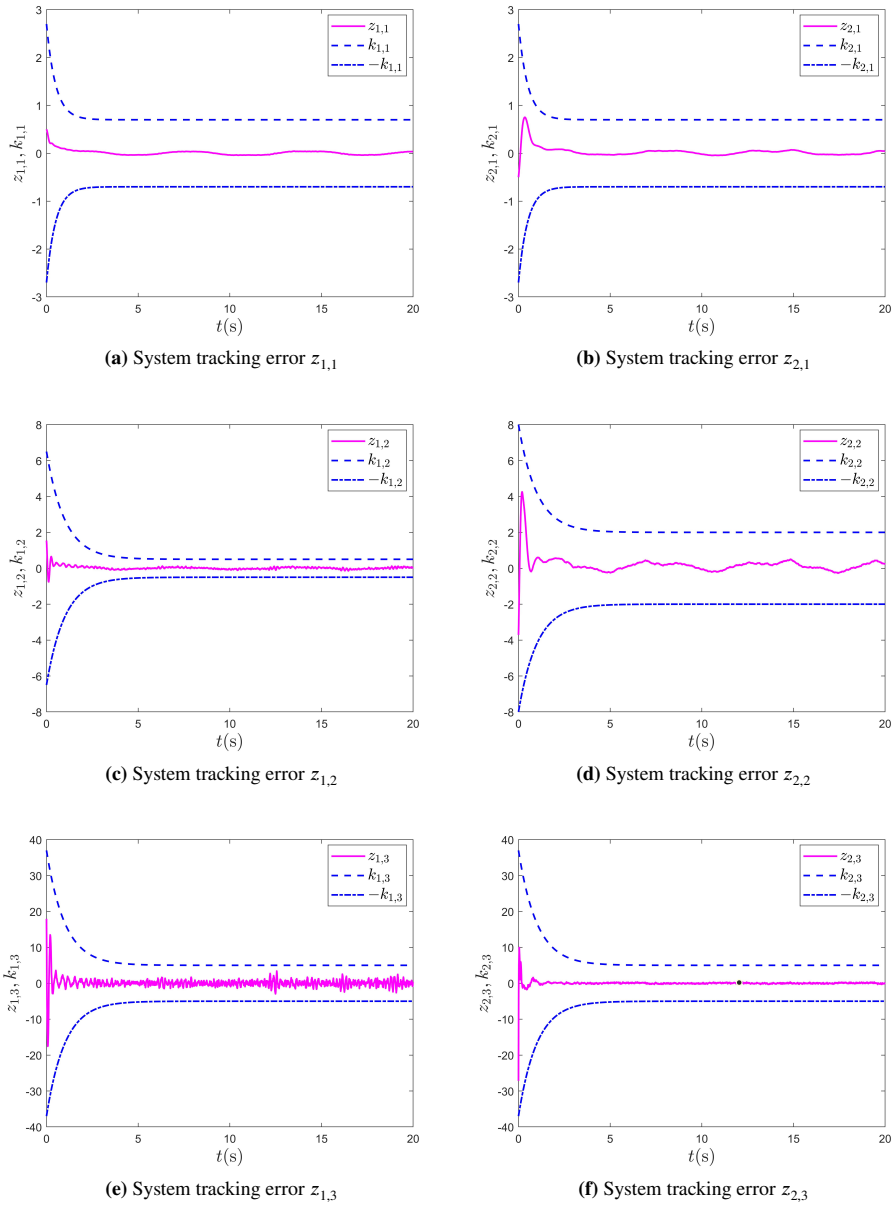


FIGURE 5 System tracking error $z_{i,j}$ ($i = 1, 2$ $j = 1, 2, 3$)

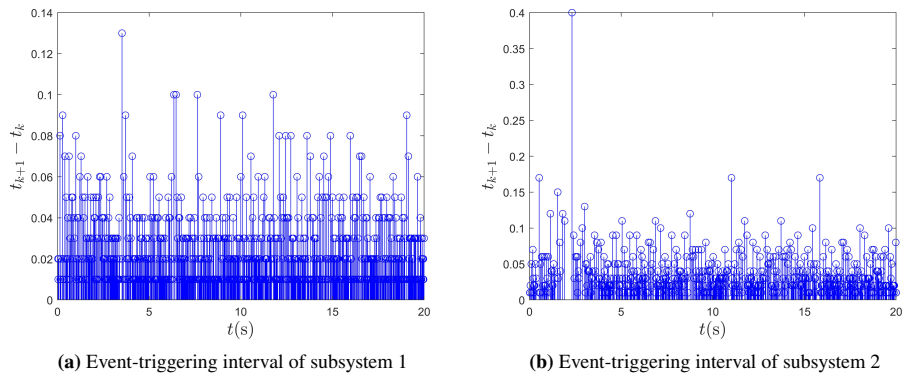


FIGURE 6 Event-triggering interval

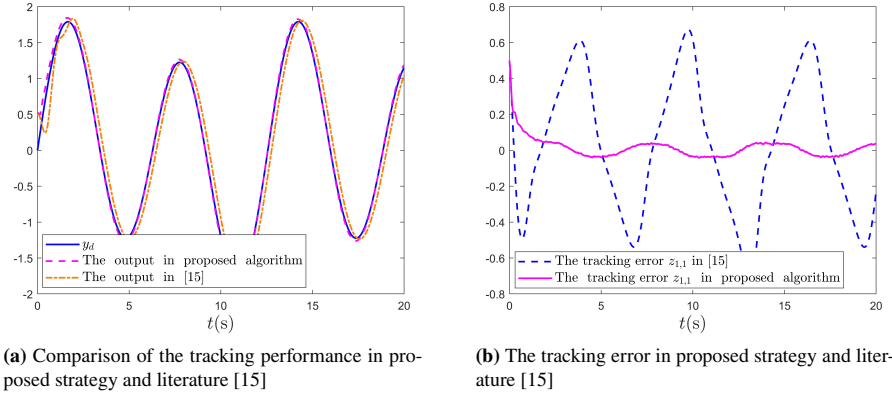


FIGURE 7 Comparative simulation

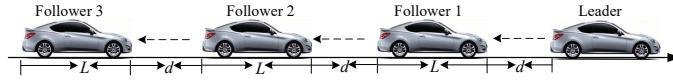


FIGURE 8 An illustration of vehicle platoon

The virtual control laws and the adaptive law are constructed as

$$\begin{aligned} \alpha_{i,1} &= -g_{i11} \frac{z_{i,1}^{\rho_1}}{h_{i,1}^{\frac{\rho_1-1}{2}}} - g_{i12} \frac{z_{i,1}^{\rho_2}}{h_{i,1}^{\frac{\rho_2-1}{2}}} - \frac{2z_{i,1}}{h_{i,1}} - \dot{k}_{i,1} + \dot{y}_{i,d} - \frac{z_{i,1}}{2c_{i,1}^2 h_{i,1}} \hat{\theta}_2 S_{i,1}^T S_{i,1} \\ \alpha_{i,2} &= -g_{i21} \frac{z_{i,2}^{\rho_1}}{h_{i,2}^{\frac{\rho_1-1}{2}}} - g_{i22} \frac{z_{i,2}^{\rho_2}}{h_{i,2}^{\frac{\rho_2-1}{2}}} - \frac{2z_{i,2}}{h_{i,2}} - \dot{k}_{i,2} - \frac{z_{i,2}}{2c_{i,2}^2 h_{i,2}} \hat{\theta}_i S_{i,2}^T S_{i,2} \\ \alpha_{i,3} &= -g_{i31} \frac{z_{i,3}^{\rho_1}}{h_{i,3}^{\frac{\rho_1-1}{2}}} - g_{i32} \frac{z_{i,3}^{\rho_2}}{h_{i,3}^{\frac{\rho_2-1}{2}}} - \frac{2z_{i,3}}{h_{i,3}} - \dot{k}_{i,3} - \frac{z_{i,3}}{2c_{i,3}^2 h_{i,3}} \hat{\theta}_i S_{i,3}^T S_{i,3} \end{aligned} \quad (84)$$

$$\dot{\hat{\theta}}_i = -\lambda_i \hat{\theta}_i + \sum_{j=1}^3 \frac{z_{i,j}^2}{2c_{i,j}^2 h_{i,j}^2} S_{i,j}^T S_{i,j} \quad (85)$$

The parameters of above equations are given as $g_{111} = g_{112} = 2$, $g_{121} = 5$, $g_{122} = 3.1$, $g_{131} = g_{132} = 5$, $g_{211} = g_{212} = 2$, $g_{221} = 5$, $g_{222} = 3.1$, $g_{231} = g_{232} = 5$, $g_{311} = g_{312} = 2$, $g_{321} = 5$, $g_{322} = 3.1$, $g_{331} = g_{332} = 5$, $c_{1,1} = c_{1,2} = c_{2,1} = c_{2,2} = c_{3,1} = c_{3,2} = 1$, $\lambda_1 = \lambda_2 = \lambda_3 = 3$, $\rho_1 = \frac{9}{11}$, $\rho_2 = \frac{11}{9}$, $\gamma_1 = \gamma_2 = \gamma_3 = 0.8$, $\eta_1 = \eta_2 = \eta_3 = 1$, $\bar{\eta}_1 = \bar{\eta}_2 = \bar{\eta}_3 = 5.01$, $\mu_1 = \mu_2 = \mu_3 = 0.2$. The body length of the vehicle is $L_i = 4\text{m}$, the desired inter-vehicle distance is $d_i = 6\text{m}$. The initial states of the vehicle platoon are chosen as $y_d = 50$, $y_v = 0$, $y_a = 0$, $x_{1,1} = 39.98$, $x_{2,1} = 29.98$, $x_{3,1} = 19.98$. The Gaussian basic function are the same as that of Example 1.

In this simulation, in order to get better results, the velocity information of the leader vehicle is taken as the reference signal. The velocity of the leader vehicle is given as

$$y_v = \begin{cases} 10 \sin\left(\frac{\pi t}{20}\right) & 0 \leq t \leq 10 \\ 10 & 10 < t < 50 \\ 10 \sin\left(\frac{\pi t}{20}\right) & 50 \leq t \leq 60 \end{cases} \quad (86)$$

TABLE 2 Number of triggering events (NTE) and transmission percentage

	Sampling times	NET	Percentage
Sub1	6000	1269	21.15%
Sub2	6000	2085	34.75%
Sub3	6000	2845	47.42%
literature [15]	6000	6000	100%

The controller is designed as

$$\Psi_i(t) = -1.8 \left[\alpha_{i,3} \tanh \left(\frac{z_{i,3} \alpha_{i,3}}{0.2 h_{1,3}} \right) + 5.01 \tanh \left(\frac{5.01 z_{i,3}}{0.2 h_{1,3}} \right) \right] \quad (87)$$

The triggering condition is defined by

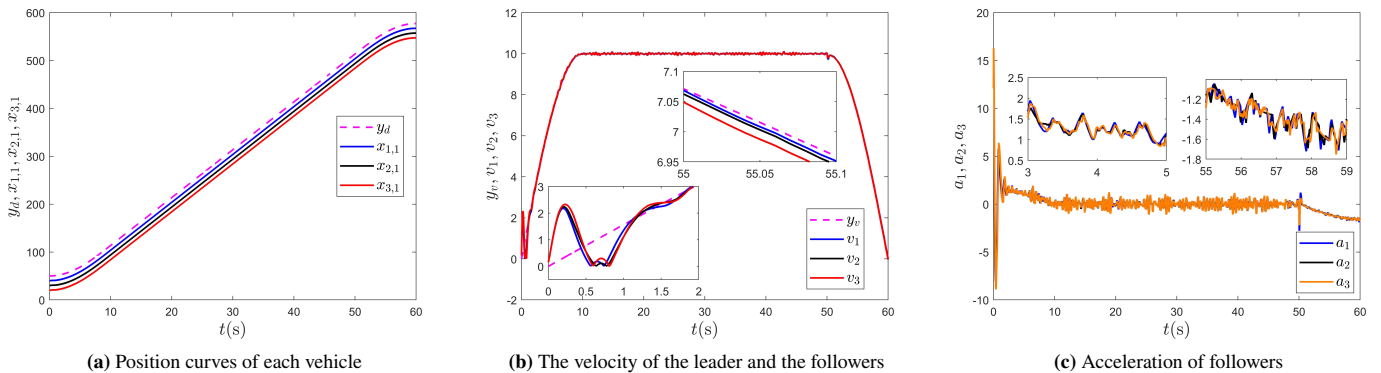
$$\begin{aligned} u_i(t) &= \Psi_i(t_k) \forall t \in [t_k, t_{k+1}) \\ t_{k+1} &= \inf \{ t > t_k \mid |e_i(t)| \geq 0.8 |\Psi_i(t_k)| + 1 \} \end{aligned} \quad (88)$$

The simulation result are shown in Fig. 9 - Fig. 12. Fig. 9 displays the position, velocity and acceleration of the vehicle platoon. Fig. 9 (a) shows the position curves of each vehicle. It is very clear that three following vehicles can track the leader well and maintain the desired inter-vehicle distance between them. Fig. 9 (b) shows the velocity of vehicles. We can see that the speed curve of the followers fluctuates slightly, and followers track the velocity of the leader vehicle well. Fig. 9 (c) is the acceleration of followers. It can be roughly seen that the acceleration is positive at first, then decreases to near zero and remains, and finally the acceleration is negative, which shows that the followers can keep up with the speed variation of the leader. In the velocity curve, the vehicle platoon accelerates first, then cruises at a constant speed, and finally decelerates.

Fig. 10 shows the tracking errors of the three following vehicles. It can be seen that all errors converge to zero after a relatively small fluctuation, and the error never exceeds the set constraint value. The three states in the simulation are position, velocity and acceleration of the vehicle. It can be seen from Fig. 9 that the states of the followers are basically consistent with that of the leader.

The control signal and output signal of the followers are displayed in Fig.11. Fig. 12 shows the event-triggered instant, obviously the duration of the trigger interval is different.

Table 2 shows the number of triggering events (NTE) and transmission percentage of three followers. Compared with time-triggered scheme, event-triggered approach obviously saves a lot of network resources. It can be seen that event-triggered strategy can improve the communication efficiency between vehicles.

**FIGURE 9** Position, velocity and acceleration of the vehicle platoon

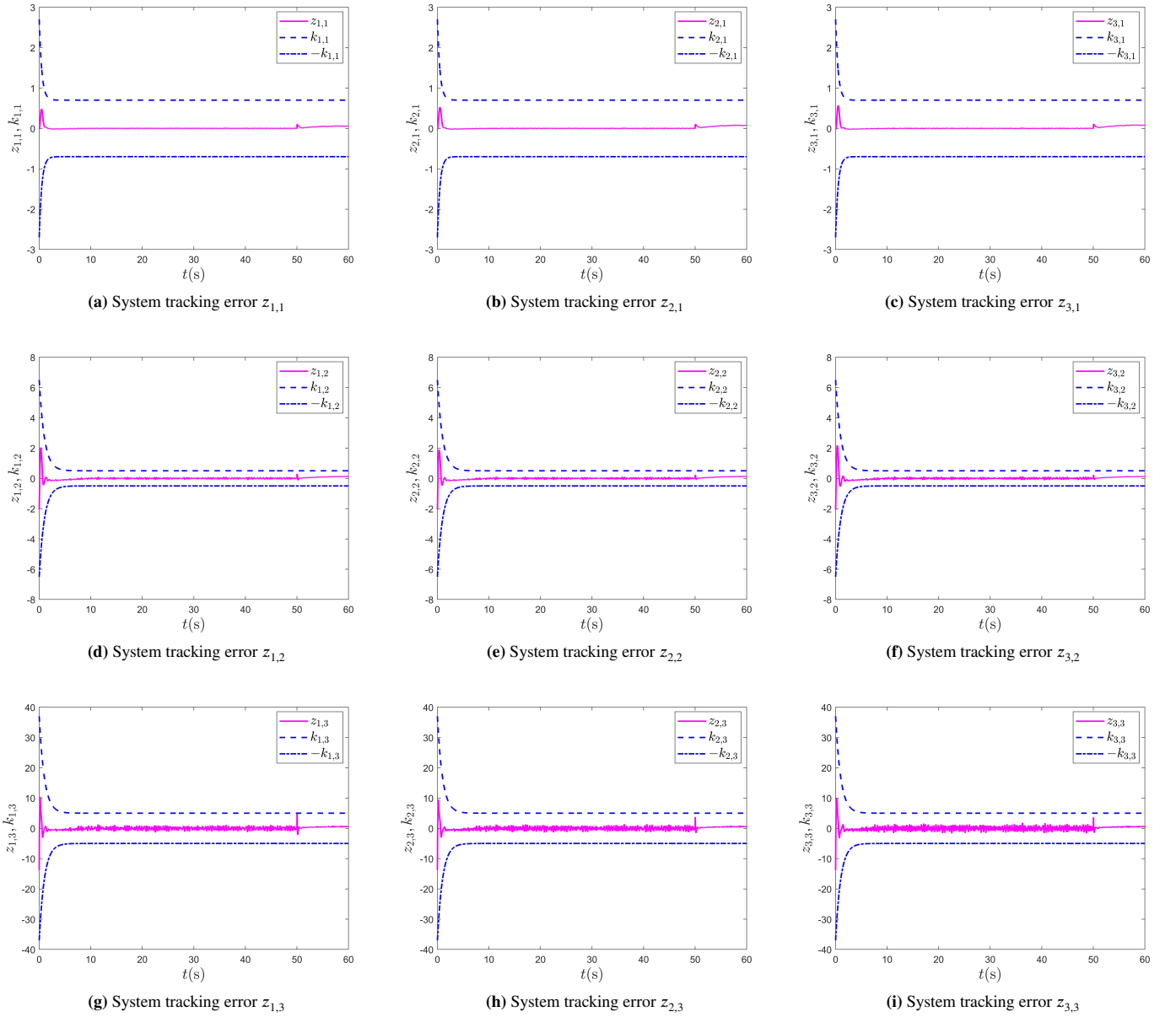


FIGURE 10 System tracking error $z_{i,j}$ ($i = 1, 2, 3$ $j = 1, 2, 3$)

5 | CONCLUSION

In this paper, the fixed time event-triggered control with state constraints has been investigated for nonlinear systems. First of all, the ETM is deployed between controller and actuator to reduce the communication burden. Then, the time-varying BLF is introduced to construct appropriate Lyapunov functions and solve the time-varying state constraint problem. Subsequently, the RBF NNs is used to solve the unknown nonlinear problems in the system. Further, the fixed time event-triggered controller is derived by backstepping technology, which can not only make the system achieve SPFTS and make the tracking error converge to a bounded set in a fixed time, but also reduce unnecessary communications. Finally, simulation results verify the feasibility and effectiveness of the proposed control strategy.

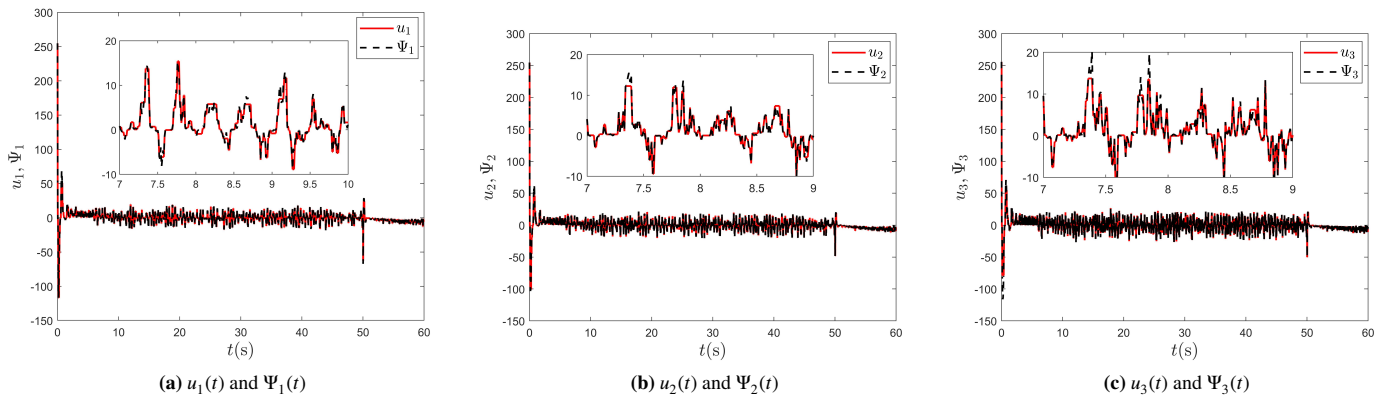


FIGURE 11 Control input of three follower

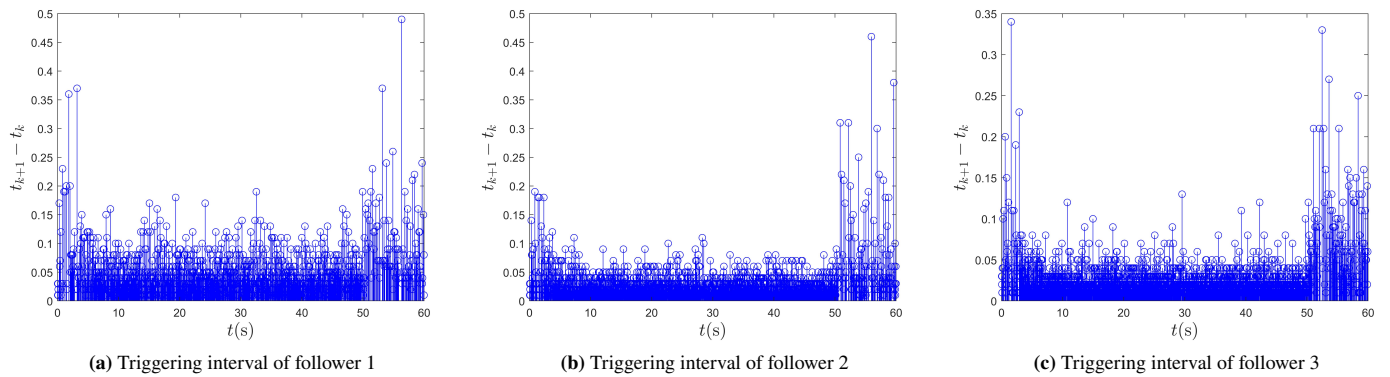


FIGURE 12 Triggering interval

References

- [1] Vargas AN, Montezuma MAF, Liu X, Xu L, Yu X. Sliding-mode control for stabilizing high-order stochastic systems: Application to one-degree-of-freedom aerial device. *IEEE Trans. Syst. Man Cybern. -Syst.* 2020; 50(11): 4318-4325. doi: 10.1109/TSMC.2018.2849846
- [2] Yu C, Xiang X, Wilson PA, Zhang Q. Guidance-error-based robust fuzzy adaptive control for bottom following of a flight-style AUV with saturated actuator dynamics. *IEEE T. Cybern.* 2020; 50(5): 1887-1899. doi: 10.1109/TCYB.2018.2890582
- [3] Patartics B, Lipták G, Luspay T, Seiler P, Takarics B, Vanek B. Application of structured robust synthesis for flexible aircraft flutter suppression. *IEEE Trans. Control Syst. Technol.* 2022; 30(1): 311-325. doi: 10.1109/TCST.2021.3066096
- [4] Xu Y, Yang H, Jiang B. Fault-tolerant control of multilayer interconnected nonlinear systems: An inclusion principle approach. *IEEE Trans. Syst. Man Cybern. -Syst.* 2021; 51(4): 2403-2414. doi: 10.1109/TSMC.2019.2912995
- [5] Guerrero J, Torres J, Creuze V, Chemori A. Observation-based nonlinear proportional-derivative control for robust trajectory tracking for autonomous underwater vehicles. *IEEE J. Ocean. Eng.* 2020; 45(4): 1190-1202. doi: 10.1109/JOE.2019.2924561
- [6] Koo M, Choi H. Output feedback regulation of a class of high-order feedforward nonlinear systems with unknown time-varying delay in the input under measurement sensitivity. *Int. J. Robust Nonlin.* 2020; 30(12): 4744-4763.
- [7] Nikiforov V, Gerasimov D, Pashenko A. Modular adaptive backstepping design with a high-order tuner. *IEEE Trans. Autom. Control* 2022; 67(5): 2663-2668. doi: 10.1109/TAC.2021.3091442

- [8] Zhang H, Lewis FL. Adaptive cooperative tracking control of higher-order nonlinear systems with unknown dynamics. *Automatica* 2012; 48(7): 1432-1439. doi: <https://doi.org/10.1016/j.automatica.2012.05.008>
- [9] Yang P, Chen X, Zhao X, Yan M. Fixed time event-triggered tracking control for interconnected nonlinear uncertain systems: An observer-based approach. *Int. J. Control Autom. Syst.* 2022; 20(8): 2641–2654.
- [10] Li Y, Tong S. Adaptive neural networks prescribed performance control design for switched interconnected uncertain nonlinear systems. *IEEE T. Neur. Net. Lear* 2018; 29(7): 3059-3068. doi: 10.1109/TNNLS.2017.2712698
- [11] Yang S, Guo Z, Wang J. Robust synchronization of multiple memristive neural networks with uncertain parameters via nonlinear coupling. *IEEE Trans. Syst. Man Cybern.- Syst* 2015; 45(7): 1077-1086. doi: 10.1109/TSMC.2014.2388199
- [12] Liu Y, Yao D, Li H, Lu R. Distributed cooperative compound tracking control for a platoon of vehicles with adaptive NN. *IEEE T. Cybern* 2022; 52(7): 7039-7048. doi: 10.1109/TCYB.2020.3044883
- [13] Zhang H, Liu Y, Wang Y. Observer-based finite-time adaptive fuzzy control for nontriangular nonlinear systems with full-state constraints. *IEEE T. Cybern* 2021; 51(3): 1110-1120. doi: 10.1109/TCYB.2020.2984791
- [14] Hong Y, Wang J, Cheng D. Adaptive finite-time control of nonlinear systems with parametric uncertainty. *IEEE Trans. Autom. Control* 2006; 51(5): 858-862. doi: 10.1109/TAC.2006.875006
- [15] Wang H, Chen B, Lin C, Sun Y, Wang F. Adaptive finite-time control for a class of uncertain high-order non-linear systems based on fuzzy approximation. *IET Contr. Theory Appl.* 2017; 11(5): 677–684.
- [16] Ju C, Son; HI. A distributed swarm control for an agricultural multiple unmanned aerial vehicle system. *Proc. Inst. Mech. Eng. Part I-J Syst Control Eng.* 2019; 233(10): 1298-1308. doi: 10.1177/0959651819828460
- [17] Zhu Y, Zheng Y, Liu X, Wang H. Fixed-time stability of positive nonlinear systems. *Trans. Inst. Meas. Control* 2020; 42(15): 2951-2955. doi: 10.1177/0142331220934608
- [18] Du H, Wen G, Wu D, Cheng Y, Lü J. Distributed fixed-time consensus for nonlinear heterogeneous multi-agent systems. *Automatica* 2020; 113: 108797. doi: <https://doi.org/10.1016/j.automatica.2019.108797>
- [19] You X, Hua C, Li K, Jia X. Fixed-time leader-following consensus for high-order time-varying nonlinear multiagent systems. *IEEE Trans. Autom. Control* 2020; 65(12): 5510-5516. doi: 10.1109/TAC.2020.3005154
- [20] Sun Y, Wang F, Liu Z, Zhang Y, Chen CLP. Fixed-time fuzzy control for a class of nonlinear systems. *IEEE T. Cybern.* 2022; 52(5): 3880-3887. doi: 10.1109/TCYB.2020.3018695
- [21] Wang L, Liu X, Cao J, Hu X. Fixed-time containment control for nonlinear multi-agent systems with external disturbances. *IEEE Trans. Circuits Syst. II-Express Briefs* 2022; 69(2): 459-463. doi: 10.1109/TCSII.2021.3091484
- [22] Yang Y, Niu Y. Fixed-time adaptive fuzzy control for uncertain non-linear systems under event-triggered strategy. *IET Control Theory A* 2020; 14(14): 1845–1854.
- [23] Qiu J, Sun K, Wang T, Gao H. Observer-based fuzzy adaptive event-triggered control for pure-feedback nonlinear systems with prescribed performance. *IEEE Trans. Fuzzy Syst.* 2019; 27(11): 2152-2162. doi: 10.1109/TFUZZ.2019.2895560
- [24] Sun W, Su SF, Wu Y, Xia J. Adaptive fuzzy event-triggered control for high-order nonlinear systems with prescribed performance. *IEEE T. Cybern* 2022; 52(5): 2885-2895. doi: 10.1109/TCYB.2020.3025829
- [25] Song C, Wang H, Tian Y, Zheng G. Event-triggered observer design for delayed output-sampled systems. *IEEE Trans. Autom. Control* 2020; 65(11): 4824-4831. doi: 10.1109/TAC.2019.2960267
- [26] Yang H, Zhao H, Xia Y, Zhang J. Event-triggered active MPC for nonlinear multiagent systems with packet losses. *IEEE T. Cybern.* 2021; 51(6): 3093-3102. doi: 10.1109/TCYB.2019.2908389
- [27] Zhou Q, Wang L, Wu C, Li H, Du H. Adaptive fuzzy control for nonstrict-feedback systems with input saturation and output constraint. *IEEE Trans. Syst. Man Cybern. -Syst.* 2017; 47(1): 1-12. doi: 10.1109/TSMC.2016.2557222

- [28] Li L, Song X. State estimation for systems with packet dropping and state equality constraints. *IEEE Trans. Circuits Syst. II-Express Briefs* 2019; 66(9): 1572-1576. doi: 10.1109/TCSII.2018.2889047
- [29] Andersson LE, Imsland L, Brekke EF, Scibilia F. On Kalman filtering with linear state equality constraints. *Automatica* 2019; 101: 467-470. doi: <https://doi.org/10.1016/j.automatica.2018.12.010>
- [30] Tee KP, Ge SS, Tay EH. Barrier Lyapunov functions for the control of output-constrained nonlinear systems. *Automatica* 2009; 45(4): 918-927. doi: <https://doi.org/10.1016/j.automatica.2008.11.017>
- [31] Yu J, Zhao L, Yu H, Lin C. Barrier Lyapunov functions-based command filtered output feedback control for full-state constrained nonlinear systems. *Automatica* 2019; 105: 71-79. doi: <https://doi.org/10.1016/j.automatica.2019.03.022>
- [32] Liu Y, Ma L, Liu L, Tong S, Chen CLP. Adaptive neural network learning controller design for a class of nonlinear systems with time-varying state constraints. *IEEE Trans. Neural Netw. Learn. Syst.* 2020; 31(1): 66-75. doi: 10.1109/TNNLS.2019.2899589
- [33] Li D, Lu S, Liu L. Adaptive NN cross backstepping control for nonlinear systems with partial time-varying state constraints and its applications to hyper-chaotic systems. *IEEE Trans. Syst. Man Cybern. -Syst.* 2021; 51(5): 2821-2832. doi: 10.1109/TSMC.2019.2917056
- [34] Sun J, Yi J, Pu Z. Fixed-time adaptive fuzzy control for uncertain nonstrict-feedback systems with time-varying constraints and input saturations. *IEEE Trans. Fuzzy Syst* 2022; 30(4): 1114-1128. doi: 10.1109/TFUZZ.2021.3052610
- [35] Yan M, Ma W, Zuo L, Yang P. Dual-mode distributed model predictive control for platooning of connected vehicles with nonlinear dynamics. *Int. J. Control Autom. Syst.* 2019; 17(12): 3091-3101.

How to cite this article: Williams K., B. Hoskins, R. Lee, G. Masato, and T. Woollings (2016), A regime analysis of Atlantic winter jet variability applied to evaluate HadGEM3-GC2, *Q.J.R. Meteorol. Soc.*, 2017;00:1–6.